CONFORMAL GEOMETRY AND DYNAMICS
An Electronic Journal of the American Mathematical Society
Volume 3, Pages 116–150 (October 25, 1999)
S 1088-4173(99)00042-9

FORD AND DIRICHLET DOMAINS FOR CYCLIC SUBGROUPS OF $PSL_2(\mathbb{C})$ ACTING ON $\mathbb{H}^3_{\mathbb{R}}$ AND $\partial\mathbb{H}^3_{\mathbb{R}}$

TODD A. DRUMM AND JONATHAN A. PORITZ

Abstract. Let Γ be a cyclic subgroup of $PSL_2(\mathbb{C})$ generated by a loxodromic element. The Ford and Dirichlet fundamental domains for the action of Γ on $\mathbb{H}^3_{\mathbb{R}}$ are the complements of configurations of half-balls centered on the plane at infinity $\partial\mathbb{H}^3_{\mathbb{R}}$. Jørgensen (*On cyclic groups of Möbius transformations*, Math. Scand. **33** (1973), 250–260) proved that the boundary of the intersection of the Ford fundamental domain with $\partial\mathbb{H}^3_{\mathbb{R}}$ always consists of either two, four, or six circular arcs and stated that an arbitrarily large number of hemispheres could contribute faces to the Ford domain in the interior of $\mathbb{H}^3_{\mathbb{R}}$. We give new proofs of Jørgensen's results, prove analogous facts for Dirichlet domains and for Ford and Dirichlet domains in the interior of $\mathbb{H}^3_{\mathbb{R}}$, and give a complete decomposition of the parameter space by the combinatorial type of the corresponding fundamental domain.

Contents

1. Introduction
2. Preliminaries
  2.1. Parabolic elements
  2.2. Elliptic elements
  2.3. Loxodromic elements
3. Fundamental domains
  3.1. Dirichlet domains
  3.2. Ford domains
  3.3. Deformations
  3.4. General notation and terminology
4. Combinatorics of fundamental domains
5. Ford and Dirichlet domains on $\partial\mathbb{H}^3_{\mathbb{R}}$
  5.1. Parabolic generators
  5.2. Elliptic generators
  5.3. Loxodromic generators
6. The decomposition of the trace plane
  6.1. Deformations, again
  6.2. Near the real axis

1991 *Mathematics Subject Classification.* Primary 20H10; Secondary 57M60, 57S30, 57S25.

Key words and phrases. Fundamental domain, Ford domain, Dirichlet domain, hyperbolic geometry.

The first author was partially supported by the Swarthmore College Research Fund.

The second author was partially supported by NSF grant DMS-9403784.

6.3. Farey sequences
6.4. The decomposition
7. Fundamental domains inside $\mathbb{H}^3$
8. Appendix: related software
References

1. Introduction

In this paper we revisit and expand upon the work of Troels Jørgensen [2], which classified the combinatorial types of Ford fundamental domains on the Riemann sphere of cyclic subgroups of $PSL_2(\mathbb{C})$ and briefly described the combinatorial types of Ford domains in $\mathbb{H}^3_{\mathbb{R}}$. Here we provide new proofs and many additional details and pictures for much of Jørgensen's work, and then we extend the discussion to an analysis of the corresponding combinatorial information for Dirichlet domains and for Ford and Dirichlet domains in the interior of hyperbolic space. In addition, we completely describe the decomposition of the parameter space for conjugacy classes of cyclic subgroups – the complex plane of traces of their generators – by the combinatorial type of the resulting fundamental domains.

Although Jørgensen stated some of the theorems that are proven here, we have relied upon computer-aided experiments to make his deep and beautiful ideas more transparent and to motivate other approaches in most cases. We have written a **Java** applet to help visualize the fundamental domains, especially on $\partial\mathbb{H}^3_{\mathbb{R}}$. We also used Davide Cervone's **StageManager** plug-in to **GeomView** to visualize the domains in $\mathbb{H}^3_{\mathbb{R}}$.

This paper is organized as follows: In §2 and §3 we give some general preliminaries on hyperbolic space and then on fundamental domains; we continue in §4 with the combinatorial facts which are the the backbone of our proofs. We look next at the combinatorics of fundamental domains on the boundary $\partial\mathbb{H}^3_{\mathbb{R}}$ in §5 and give the corresponding decomposition of the trace plane in §6. Finally, in §7, we provide a complete combinatorial description of fundamental domains in the interior of $\mathbb{H}^3_{\mathbb{R}}$. An appendix following the main part of the paper as §8 explains the algorithms and user controls of the visualization applet mentioned above; in the electronic version of this paper, the applet itself is available from the page containing the abstract, and the user is encouraged to consult the applet while reading the proofs and explanations in the article.

In addition to acknowledging the invaluable help we received from **The Geometry Center** and its staff, especially Robert Miner and Davide Cervone, we would like to thank Bill Goldman and Al Marden for bringing this project to our attention. Programming assistance was also provided by Adam Rosien and Wajeeha Naeem.

2. Preliminaries

We shall work with the upper half-space model of hyperbolic 3-space in either of the two forms:

$$\mathbb{H}^3 = \{(z,t) \in \mathbb{C} \times \mathbb{R} \mid t > 0\} = \{(x_1,x_2,x_3) \in \mathbb{R}^3 \mid x_3 > 0\}.$$

Its boundary is the Riemann sphere $\widehat{\mathbb{C}} = \mathbb{C} \cup \infty$; we shall sometimes work in $\overline{\mathbb{H}^3} = \mathbb{H}^3 \cup \widehat{\mathbb{C}}$, which is given the topology of a closed unit ball. For a more complete discussion of hyperbolic 3-space than we shall present here, the reader is referred to [1].

The hyperbolic distance $\rho(x, y)$ between points $x, y \in \mathbb{H}^3$ is determined by

$$\cosh \rho(x, y) = 1 + \frac{\|x - y\|^2}{2x_3 y_3}, \tag{2.1}$$

where $\|\cdot\|$ denotes the Euclidean norm on $\mathbb{R}^3$.

The group of orientation preserving isometries of $\mathbb{H}^3$ can be identified with $PSL_2(\mathbb{C})$, which consists of equivalence classes of matrices in $SL_2(\mathbb{C})$ up to sign. We shall usually ignore this problem of sign and work with a representative in $SL_2(\mathbb{C})$ (the representative whose trace has positive imaginary part when convenient); statements we make about matrices will thus always be invariant under change of sign or true after the appropriate sign is chosen. For example, a given element

$$\gamma = \begin{bmatrix} a & b \\ c & d \end{bmatrix} \in PSL_2(\mathbb{C}) \tag{2.2}$$

acts by fractional linear transformations on $\widehat{\mathbb{C}}$ and as the isometry

$$\gamma : (z, t) \mapsto \left(\frac{(az + b)\overline{(cz + d)} + a\bar{c}t^2}{|cz + d|^2 + |c|^2 t^2}, \frac{t}{|cz + d|^2 + |c|^2 t^2} \right) \tag{2.3}$$

of $\mathbb{H}^3$, both of which actions are independent of the overall sign of the representative. On the other hand, when we say that the elements of $PSL_2(\mathbb{C})$ are classified by their trace $\tau(\gamma) = a + d$, it is in the sense that two elements with representatives whose traces differ only by a sign are conjugate in $PSL_2(\mathbb{C})$ (and certainly two conjugate elements of $PSL_2(\mathbb{C})$ have representatives with the same trace).

We now recall the famous partition of $PSL_2(\mathbb{C})$ into parabolic, elliptic and loxodromic elements.

2.1. **Parabolic elements.** A non-identity element γ is called *parabolic* if $\tau(\gamma) = \pm 2$. All parabolic elements are conjugate, and we usually use the following representative, which fixes the point 0 in $\widehat{\mathbb{C}}$:

$$\gamma = \begin{bmatrix} 1 & 0 \\ 1 & 1 \end{bmatrix}, \text{ noting that } \gamma^n = \begin{bmatrix} 1 & 0 \\ n & 1 \end{bmatrix}. \tag{2.4}$$

2.2. **Elliptic elements.** A non-identity element γ is called *elliptic* if its trace is real and bounded between -2 and 2. An elliptic element

- has complex eigenvalues,
- fixes a geodesic (and its endpoints) pointwise and
- acts as a rotation about this fixed geodesic.

In our computations we shall conjugate all elliptic elements so that their fixed geodesic has endpoints 0 and 1 in $\widehat{\mathbb{C}}$ and are hence of the form:

$$\gamma = \begin{bmatrix} e^{i\theta} & 0 \\ e^{i\theta} - e^{-i\theta} & e^{-i\theta} \end{bmatrix} = \begin{bmatrix} \lambda & 0 \\ \beta_1 & \lambda^{-1} \end{bmatrix}, \text{ noting that } \gamma^n = \begin{bmatrix} \lambda^n & 0 \\ \beta_n & \lambda^{-n} \end{bmatrix}, \tag{2.5}$$

where

$$\beta_n = \lambda^n - \lambda^{-n} = e^{ni\theta} - e^{-ni\theta} = 2i \sin(n\theta). \tag{2.6}$$

(This notation is due to Jørgensen [2].) In this case, the trace $\tau_n = \tau(\gamma^n) = 2\cos(n\theta)$.

Note that a γ in the form (2.5) rotates the hyperbolic planes perpendicular to its fixed geodesic by an angle of 2θ, so it is only geometrically interesting to consider these elements when $\theta \in (0, \pi)$.

2.3. **Loxodromic elements.** A non-identity element γ is called *loxodromic* if it is neither elliptic or parabolic: A loxodromic element

- has eigenvalues whose norms are $\neq 1$,
- fixes a geodesic in $\mathbb{H}^3$, called its *axis*,
- acts as a translation along its axis, along with a rotation around the axis and
- is called *hyperbolic* if its trace is real (and hence there is no rotation around the axis).

The endpoints of the axis are fixed points for the action of γ. The endpoint a for which $\lim_{n\to\infty} \gamma^n x = a$ for any $x \in \mathbb{H}^3$ is called the *attracting fixed point.* The endpoint b for which $\lim_{n\to-\infty} \gamma^n x = b$ for any $x \in \mathbb{H}^3$ is called the *repelling fixed point.*

To simplify computations, we shall choose representatives of loxodromic conjugacy classes whose attracting fixed point is 1 and whose repelling fixed point is 0:

$$\gamma = \begin{bmatrix} \lambda & 0 \\ \beta_1 & \lambda^{-1} \end{bmatrix}, \text{ noting that } \gamma^n = \begin{bmatrix} \lambda^n & 0 \\ \beta_n & \lambda^{-n} \end{bmatrix}, \tag{2.7}$$

where again

$$\beta_n = \lambda^n - \lambda^{-n}. \tag{2.8}$$

This representative can be computed from the trace $\tau = \lambda + \lambda^{-1}$ by defining it to be as in (2.7) with λ given by

$$\lambda = \frac{\tau \pm \sqrt{\tau^2 - 4}}{2},$$

with the sign chosen so that $|\lambda| > 1$, *i.e.*, 1 is chosen to be the attracting fixed point. Let us use as branch cut in the complex square root the positive real axis, so that the function

$$\lambda(\tau) = \frac{\tau + \sqrt{\tau^2 - 4}}{2}, \tag{2.9}$$

will be discontinuous only along the two segments $(-\infty, -2)$ and $(2, \infty)$ on the real axis. Furthermore, if this λ has modulus one, then it is of the form $\lambda = e^{i\theta}$, so

$$2\cos\theta = e^{i\theta} + e^{-i\theta} = \lambda + \lambda^{-1} = \tau.$$

That is, $|\lambda(\tau)| = 1$ if and only if τ is in the segment $[-2, 2]$ on the real axis. Since $|\lambda(i)| = \left|\frac{(1+\sqrt{5})i}{2}\right| > 1$, it follows that the formula (2.9) defines the desired λ from τ in a way that is continuous on the upper half-plane union the segment $[-2, 2]$ on the real axis. The limiting γ that results as τ approaches this real segment is the corresponding elliptic element; in particular, it is important to remember that as $\tau \to \pm 2$ the $\gamma \to \mathrm{Id}$, which differs slightly from our convention above that $\tau = \pm 2$ is the trace representing the parabolic element (2.4).

Finally, note that if we set $\tau_n = \tau(\gamma^n)$, then $\tau_n = \lambda^n + \lambda^{-n}$ and $\beta_n = \sqrt{\tau_n^2 - 4}$. Using this common notation has the pleasant side effect that with γ^n in the standard forms we have chosen for elliptic or loxodromic elements, the hyperbolic isometry (2.3) takes the point $(\frac{1}{2}, \frac{t}{2})$ to the point

$$\gamma^n \left(\frac{1}{2}, \frac{t}{2}\right) = \left(\frac{\lambda^n \overline{(\tau_n + \beta_n t^2)}}{D_n}, \frac{2t}{D_n}\right), \tag{2.10}$$

where

$$D_n = |\tau_n|^2 + |\beta_n|^2 t^2. \tag{2.11}$$

This will be useful in computing Dirichlet domains, below.

3. Fundamental domains

The Dirichlet and Ford domains in $\mathbb{H}^3$, defined below, are both fundamental domains for the action of group Γ on $\mathbb{H}^3$ bounded by Euclidean hemispheres. By abuse of terminology, we define the Dirichlet (respectively, Ford) domains on $\partial\mathbb{H}^3 = \widehat{\mathbb{C}}$ to be the intersection of the boundary of the Dirichlet (respectively, Ford) domain and $\widehat{\mathbb{C}}$.

It can be shown that for a group which does not fix ∞, the Ford domain is the limit of the Dirichlet domains as the basepoint of the Dirichlet domain tends towards ∞. We shall prove this below for cyclic groups Γ.

3.1. **Dirichlet domains.** The *Dirichlet domain* Δ_Γ^x *for the action of* Γ *on* $\mathbb{H}^3$ *based at* $x \in \mathbb{H}^3$ is the set of points

$$\{y \in \mathbb{H}^3 \mid \rho(y, x) \leq \rho(y, \gamma x) \ \forall \gamma \in \Gamma\},$$

while, with a slight abuse of notation and terminology, we shall say that the *Dirichlet domain* $\widehat{\Delta}_\Gamma^x$ *for the action of* Γ *on* $\widehat{\mathbb{C}}$ *based at* $x \in \mathbb{H}^3$ is the set $\Delta_\Gamma^x \cap \widehat{\mathbb{C}}$ minus any fixed points of Γ on $\widehat{\mathbb{C}}$. Δ_Γ^x is bounded by hyperbolic planes which are equidistant between x and its images γx for all $\gamma \in \Gamma$ not fixing x; in the upper half-space model of $\mathbb{H}^3$, these planes are Euclidean hemispheres centered on $\partial\mathbb{H}^3$.

Consider $x = (z, t)$ and $y = (w, s)$ as points in $\mathbb{H}^3 = \mathbb{C} \times \mathbb{R}^+$. The equidistant surface $E(x, y)$ has center $C^{eq}(x, y)$ and radius $R^{eq}(x, y)$ given by

$$\begin{aligned} C^{eq}((z,t),(w,s)) &= (tw - sz)/(t-s) \qquad \text{and} \\ R^{eq}((z,t),(w,s)) &= \sqrt{ts\left(1 + |z-w|^2/(t-s)^2\right)}. \end{aligned} \tag{3.1}$$

For any $g \in PSL_2(\mathbb{C})$, we note that

$$g\left(\Delta_\Gamma^x\right) = \Delta_{g\Gamma g^{-1}}^{gx}.$$

This transformation does not change the configuration of equidistant surfaces which make up the boundary of the Dirichlet domain, so we only need discuss the combinatorial type for one conjugate of the group Γ. For the cyclic groups $\Gamma = \langle\gamma\rangle$ we are considering in this paper, we may thus assume that γ is in one of our preferred forms as in §2, and use all of the formulæ there. In fact, conjugating by elements which fix 0 and 1 does not change our preferred forms of γ; as $PSL_2(\mathbb{C})$ contains elements fixing 0 and 1 and rotating around or translating along (by an arbitrary amount) the geodesic connecting 0 and 1, we can move any basepoint to any other as long as its distance to this geodesic is unchanged, still keeping γ in the desired form.

For our analysis of Dirichlet domains of non-parabolic groups, we shall use the basepoint

$$x = (z,t) = \left(\frac{1}{2}, \frac{e^{\rho}}{2}\right), \tag{3.2}$$

whose hyperbolic distance to the geodesic joining 0 and 1 is ρ. Plugging the formula (2.10) for the image of this basepoint under γ^n into the above equation (3.1) for equidistant surfaces, we find that the center and radius of the equidistant surface $E_n = E(x, \gamma^n x)$ are

$$\begin{array}{rcll} C_n^{eq} & = & \frac{\lambda^n \overline{(\tau_n + \beta_n e^{2\rho})} - 2}{D_n - 4} & \text{and} \\ R_n^{eq} & = & \sqrt{\frac{e^{2\rho}}{D_n}\left(1 + \frac{\left|2\lambda^n \overline{(\tau_n + \beta_n e^{2\rho})} - D_n\right|^2}{e^{2\rho}(D_n-4)^2}\right)}, & \text{where} \\ D_n & = & |\tau_n|^2 + |\beta_n|^2 e^{2\rho}. & \end{array} \tag{3.3}$$

We shall write $\widehat{E}_n$ for the boundary of the equidistant surface E_n in $\widehat{\mathbb{C}}$; it is a circle with center C_n^{eq} and radius R_n^{eq}.

3.2. **Ford domains.** Given an element $\gamma \in PSL_2(\mathbb{C})$ which does not fix ∞, there exists a unique pair of *isometric hemispheres* $I_{\gamma^{\pm 1}}$ centered on $\partial\mathbb{H}^3$ such that γ acts as an Euclidean isometry from $I_{\gamma^{-1}}$ to I_γ. The boundaries of the isometric hemispheres are called *isometric circles* and are denoted $\widehat{I}_{\gamma^{\pm 1}}$; γ also takes $\widehat{I}_{\gamma^{-1}}$ to $\widehat{I}_\gamma$ as an Euclidean isometry. For an arbitrary element γ as above in (2.2), the center and radius of both the isometric hemispheres and circles are as follows:

$$\begin{array}{rcl} C^{iso}(\gamma) & = & a/c \\ R^{iso}(\gamma) & = & 1/|c|. \end{array} \tag{3.4}$$

More specifically, for elements γ given in one of the preferred forms of §2 the centers and radii of the isometric circles for the powers of γ are given by

$$\begin{array}{rcccll} C_n^{iso} & = & C^{iso}(\gamma^n) & = & \lambda^n/\beta_n & \text{and} \\ R_n^{iso} & = & R^{iso}(\gamma^n) & = & 1/|\beta_n|. & \end{array} \tag{3.5}$$

If the group Γ has no non-identity elements that fix ∞, we define the *Ford domain* Δ_Γ^∞ *for the action of* Γ *on* $\mathbb{H}^3$, to be the closure of the intersection of the exteriors of the isometric hemispheres of the non-identity elements of Γ minus any fixed points of Γ. We also call the intersection of the exteriors of the isometric circles for all non-identity elements of Γ minus any fixed points of Γ the *Ford domain* $\widehat{\Delta}_\Gamma^\infty$ *for the action of* Γ *on* $\widehat{\mathbb{C}}$.

We note here that the limit of the expressions in (3.3) as $\rho \to \infty$ results in the expressions in (3.5). Ford domains can thus be viewed as the "limit of Dirichlet domains as the center goes to ∞," and this motivated our notation Δ_Γ^∞ for Ford domains.

3.3. **Deformations.** Many of our arguments below rely upon varying the trace of γ and observing how the combinatorics of the resulting fundamental domains change. Crucial in such deformations is the fact that the centers and radii of the equidistant and isometric hemispheres are continuous functions of the trace as it moves throughout the complex upper half-plane $\mathcal{U}$ union the real interval $[-2, 2]$. More precisely,

Proposition 3.1. *Fix any $n \neq 0$ and define the set*

$$\mathcal{D}_n = \left\{ 2\cos\frac{k\pi}{n} \mid k \in \mathbb{Z} \right\} \subset [-2,2] \subset \mathbb{C}.$$

As functions of the trace, C_n^{eq}, R_n^{eq}, C_n^{iso} and R_n^{iso} are continuous on $\mathcal{C}_n = \mathcal{U} \cup ([-2,2] \setminus \mathcal{D}_n)$, while as $\tau \in \mathcal{C}_n$ tends to a point of $\mathcal{D}_n$, $\lim R_n^{eq} = \lim R_n^{iso} = \infty$.

Proof. This follows from the continuity of $\lambda(\tau)$ on the $\mathcal{U} \cup [-2,2]$ and the fact that the centers and radii are rational functions of the real and imaginary parts of λ with well-defined finite values for $\tau \in \mathcal{C}_n$. The points of $\mathcal{D}_n$ are instead exactly those for which $\lambda^n = 1$ so that $\gamma^n = \mathrm{Id}$ and the nth isometric and equidistant circles are undefined. Where positive rational functions such as R_n^{eq} and R_n^{iso} are undefined they have limit infinity, as claimed. □

In the sequel, we shall use the term *deformation* for a change in τ which is as small as necessary to apply the above continuity to the situation at hand.

3.4. **General notation and terminology.** For the remainder of this paper, the following conventions shall be in force:

- $\mathcal{U}$ is the upper complex half-plane;
- $\Gamma = \langle\gamma\rangle$ where γ is not elliptic of infinite order;
- Δ is the Ford or Dirichlet domain for the action of Γ on $\mathbb{H}^3$;
- X_n is the n^{th} isometric or equidistant hemisphere in $\mathbb{H}^3$, depending on the type of Δ;
- $\widehat{\Delta}$ and $\widehat{X}_n$ are the corresponding objects in $\widehat{\mathbb{C}}$;
- the *interior* (respectively, *exterior*) of X_n is the bounded (respectively, unbounded) component of $\mathbb{H}^3 \setminus X_n$, and likewise for $\widehat{X}_n$;
- $\overline{\Delta} = \Delta \cup \widehat{\Delta}$ and $\overline{X}_n = X_n \cup \widehat{X}_n$ in $\overline{\mathbb{H}^3}$;
- $X_n^\partial = X_n \cap \partial\Delta$, $\widehat{X}_n^\partial = \widehat{X}_n \cap \partial\widehat{\Delta}$ and $\overline{X}_n^\partial = X_n^\partial \cup \widehat{X}_n^\partial$;
- a *face* F_n is a non-empty maximal connected 2-dimensional subset of X_n^∂;
- an *edge* $E_{i,j}$ is the non-empty 1-dimensional intersection of the faces F_i and F_j;
- a *vertex* V is the non-empty 0-dimensional intersection of three or more faces;
- a *side* S_n is a non-empty maximal connected 1-dimensional subset of $\widehat{X}_n^\partial$; and
- a *corner* C is the non-empty 0-dimensional intersection of at least two sides.

We shall use the superscripts *eq* and *iso* when necessary to differentiate between equidistant and isometric faces, sides, etc.

4. Combinatorics of fundamental domains

We now address some of the combinatorial properties of the Ford and Dirichlet domains of a cyclic group. It is fundamental here that γ^n maps $\overline{X}_{-n}$ to $\overline{X}_n$ taking the exterior of X_{-n} to the interior of X_n. This implies first that γ^n identifies points on $\partial\overline{\Delta}$ if and only if they are actually on $\overline{X}_{\pm n}$:

Proposition 4.1. *If $\gamma^n p = q$ for $p, q \in \partial\overline{\Delta}$, then $p \in \overline{X}_{-n}$ and $q \in \overline{X}_n$.*

Proof. If p were external to X_{-n}, then $\gamma^n p$ would be internal to X_n, contradicting the fact that $\gamma^n p = q \in \partial\Delta$. Hence p is on or inside X_{-n} and so q is on or outside X_n. Applying the same reasoning with γ^{-n} yields the other containment, and exactly the same argument applies on $\widehat{\mathbb{C}}$ to yield the result also for $\widehat{\Delta}$. □

Our next proposition is something of a converse to the previous one.

Proposition 4.2. *For any* $n \neq 0$, $\gamma^{-n}\,\overline{X}_n^\partial = \overline{X}_{-n}^\partial$.

Proof. We shall only prove this for the Dirichlet domain inside $\mathbb{H}^3$, the other cases following easily.

Let $x \in \mathbb{H}^3$ be the basepoint of Δ. From the definition of a Dirichlet domain, we can write

$$X_n^\partial = \{y \in \mathbb{H}^3 \mid \rho(y,x) = \rho(y,\gamma^n\,x) \le \rho(y,\gamma^m\,x)\ \forall m\}.$$

Hence

$$\begin{aligned}\gamma^{-n}\,X_n^\partial &= \{y \in \mathbb{H}^3 \mid \rho(\gamma^n\,y,x) = \rho(\gamma^n\,y,\gamma^n\,x) \le \rho(\gamma^n\,y,\gamma^m\,x)\ \forall m\}\\ &= \{y \in \mathbb{H}^3 \mid \rho(y,\gamma^{-n}\,x) = \rho(y,x) \le \rho(y,\gamma^{m-n}\,x),\ \forall m\}\\ &= \{y \in \mathbb{H}^3 \mid \rho(y,x) = \rho(y,\gamma^{-n}\,x) \le \rho(y,\gamma^k\,x),\ \forall k\} = X_{-n}^\partial.\end{aligned}$$

□

There is special symmetry for Ford and Dirichlet domains of cyclic groups generated by elliptic or loxodromic generators. Let ϕ be the orientation-preserving diffeomorphism of $\mathbb{H}^3$ given by

$$\phi : (z,t) \mapsto (1-z,t).$$

Then a simple calculation with the action (2.3) yields

Proposition 4.3. *If* γ *fixes* 0 *and* 1*, then* $\phi^{-1} \circ \gamma \circ \phi = \gamma^{-1}$ *as diffeomorphisms of* $\mathbb{H}^3$*. Hence if* Δ *is a Ford or Dirichlet domain for* $\Gamma = \langle\gamma\rangle$*, then* ϕ *preserves* Δ *and in fact interchanges faces* $F_{\pm n}$*, edges* $E_{i,j}$ *and* $E_{-i,-j}$*, etc., and likewise on* $\widehat{\mathbb{C}}$*.*

In Propositions 4.3 and 4.2 we see that ϕ and γ^n both map F_{-n} to its inverse face F_n; however, ϕ is orientation-preserving while γ^n reverses orientation. Here we are giving the hemispheres $X_{\pm n}$ the outward-pointing orientation and then inducing an orientation on their subsets $F_{\pm n}$. Thus since γ^n takes the interior of X_{-n} to the exterior of X_n, as was observed above, it reverses the orientation of the faces, while ϕ does not because it is merely a rotation around a vertical line.

We first apply these propositions to the case when the two hemispheres $\overline{X}_n$ and $\overline{X}_m$ both meet $\partial\overline{\Delta}$ in a single point p. By Proposition 4.2, $\overline{X}_{-n}$ meets $\partial\overline{\Delta}$ at the single point $\gamma^{-n}\,p$ and $\overline{X}_{-m}$ meets $\partial\overline{\Delta}$ at the single point $\gamma^{-m}\,p$; see Figure 4.1 for an example on $\widehat{\mathbb{C}}$. However, by Proposition 4.3, $\gamma^{-n}\,p = \phi(p) = \gamma^{-m}\,p$. Since the fixed points of loxodromic γ are not included in $\partial\overline{\Delta}$, we have the following

Proposition 4.4. *If* γ *is loxodromic and* $\overline{X}_n^\partial = \overline{X}_m^\partial$ *is a single point, then* $n = m$*.*

We also know that if $\overline{X}_n$ and $\overline{X}_m$ meet at an edge, vertex, or corner, then $\overline{X}_{n-m}$ also has a non-empty intersection with the boundary of the fundamental domain.

Proposition 4.5. *If* $\overline{X} = \overline{X}_n^\partial \cap \overline{X}_m^\partial \neq \emptyset$ *for* $n \neq m$*, then* $\emptyset \neq \gamma^{-m}\,\overline{X} \subset \overline{X}_{(n-m)}^\partial$ *and* $\emptyset \neq \gamma^{-n}\,\overline{X} \subset \overline{X}_{(m-n)}^\partial$*.*

Proof. By Proposition 4.2, $\gamma^{-n}\overline{X}$ and $\gamma^{-m}\overline{X}$ are subsets of $\partial\overline{\Delta}$. Since $\gamma^{n-m}(\gamma^{-n}\overline{X}) = \gamma^{-m}\,\overline{X}$, Proposition 4.1 gives our stated conclusion. □

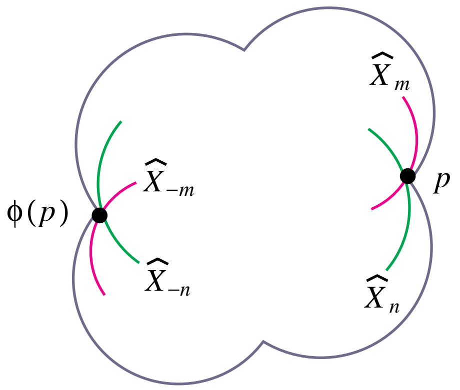

FIGURE 4.1. $\widehat{X}_n^\partial = \widehat{X}_m^\partial$ is a single point

We now turn our attention to tangency of X_n's. This turns out only to be an interesting issue for loxodromic generators γ, so we shall assume we are in that case for the remainder of this section. Further, since all $\overline{X}_n$'s are centered on $\widehat{\mathbb{C}}$, any point of tangency will also lie on $\widehat{\mathbb{C}}$. So we shall also now restrict our attention to $\widehat{X}_n$'s and $\widehat{\Delta}$, objects which lie on $\widehat{\mathbb{C}}$.

Our conventions for loxodromic γ imply that 1 is in the interior and 0 the exterior of $\widehat{X}_n$ when $n > 0$. Thus if $\widehat{X}_n$ and $\widehat{X}_m$ are externally tangent, then n and m must be of different signs. If $\widehat{X}_n$ is internally tangent to $\widehat{X}_m$, then n and m are of the same sign and $|n| > |m|$.

It is convenient to make the following

Definition 4.6. A point $p \in \partial\widehat{\Delta}$ is a *smooth point of the boundary* if p lies in the interior of a side.

It is possible for a smooth point p of the boundary to be in the interior of two sides S_n and S_m which are externally tangent at p. It is also possible that p is a corner and a smooth point of the boundary, such as when there exists an X_n which is internally tangent to a side at p.

Proposition 4.7. *Suppose γ is loxodromic.*

(a) *If $\widehat{X}_m$ is internally tangent to S_n at a smooth point p and $m > n > 0$, then $m = 2n$.*

(b) *If S_k is externally tangent to S_n at a smooth point q, then $k = -n$ and $q = \frac{1}{2} \in \widehat{\mathbb{C}}$.*

Furthermore, if either one of these cases occurs, then the other one also occurs and $\gamma^{-n} p = q$.

Proof. Suppose that $m > n > 0$ and $\widehat{X}_m$ is internally tangent to the side S_n at a smooth point p.

By Proposition 4.3, $\widehat{X}_{-m}$ is internally tangent to the side S_{-n} at the smooth point t which, by Proposition 4.2 must be the point $\gamma^{-m} p$. Further, $q = \gamma^{-n} p$ is a smooth point on S_{-n}. $\gamma^{m-n} t = q$ and by Proposition 4.1 this implies that $q \in \widehat{X}_{m-n}$ and $t \in \widehat{X}_{n-m}$. Since t is a smooth point of S_{-n}, either $\widehat{X}_{n-m}$ contains or is internally tangent to S_{-n}; see Figure 4.2. The latter is impossible, since either

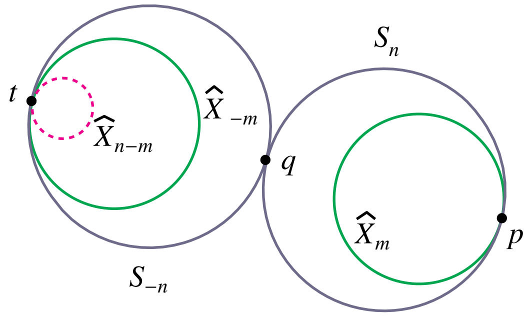

FIGURE 4.2. Part (a) of Proposition 4.7

$\widehat{X}_{-m}$ is the same as $\widehat{X}_{n-m}$, contradicting $n > 0$, or else Proposition 4.4 tells us that $-m = n - m$, yielding the same contradiction. Hence $S_{-n} \subseteq \widehat{X}_{n-m}$ and thus $m = 2n$, proving (a).

But now q is both a smooth point of S_{-n} and on $\widehat{X}_{m-n} = \widehat{X}_n$, so it must be a point of external tangency of these two curves. Applying the involution ϕ, we see that q must be a smooth point of external tangency of the sides S_{-n} and S_n, putting us in the situation of part (b).

Now suppose that S_k is externally tangent to S_n at a smooth point q. We certainly know that k and n have opposite signs, so let us assume that $k < 0 < n$. By Proposition 4.3, $q' = \phi(q)$ is a smooth point where S_{-k} and S_{-n} are externally tangent. Let $p = \gamma^n q'$ and $t = \gamma^k q'$. These are smooth points of S_n and S_k, respectively, and $\gamma^{n-k} t = p$; see Figure 4.3. From Proposition 4.1 this means that $p \in \widehat{X}_{n-k}$. On the other hand, the smoothness of S_n at p implies that $\widehat{X}_{n-k}$ must be internally tangent to S_n at p. By part (a), we have that $n - k = 2n$, so $n = -k$. This in turn implies that $q' = q$ and both equal $\frac{1}{2}$, since that is the only fixed point for ϕ on $\widehat{\mathbb{C}}$. $\square$

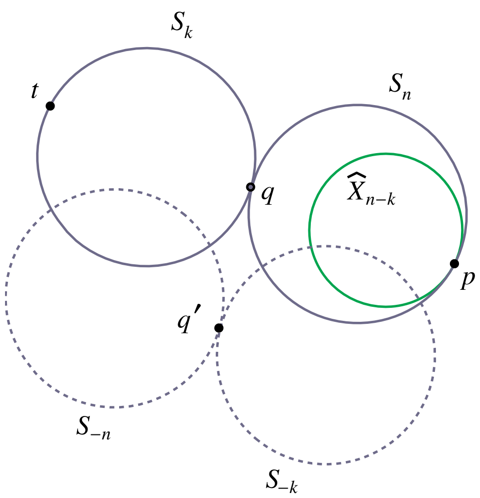

FIGURE 4.3. An impossible picture for part (b) of Proposition 4.7

5. Ford and Dirichlet domains on $\partial\mathbb{H}^3_{\mathbb{R}}$

The combinatorial types of Ford domains on $\widehat{\mathbb{C}}$ were originally classified by Jørgensen.

Theorem 5.1 (Jørgensen, [2])**.** *For a non-elliptic element $\gamma \in PSL_2(\mathbb{C})$ which does not fix ∞, the Ford domain on $\partial\mathbb{H}^3_{\mathbb{R}}$ of $\Gamma = \langle\gamma\rangle$ has two, four or six sides.*

In this section, we shall use the general combinatorial properties discovered in Section 4 to examine in some detail both Ford and Dirichlet domains. Along the way we shall extend the result of Jørgensen to Dirichlet domains of cyclic groups:

Theorem 5.2. *For $\gamma \in PSL_2(\mathbb{C})$ which is not elliptic of infinite order and does not fix ∞, the Ford and Dirichlet domains on $\partial\mathbb{H}^3_{\mathbb{R}}$ of $\Gamma = \langle\gamma\rangle$ have two, four or six sides.*

The domains look quite different for parabolic, elliptic and loxodromic generators, so we shall examine each of these cases separately.

5.1. **Parabolic generators.** Let γ be a parabolic element written as in (2.4). If we use the basepoint $(0, t)$ for Dirichlet domains, then both equidistant and isometric hemispheres have center $1/n$ and radius $1/|n|$. Hence both types of domain on $\widehat{\mathbb{C}}$ are bounded by the circles $\widehat{X}_{-1}$ and $\widehat{X}_1$, which intersect at 0. Thus our fundamental domains corresponding to $\tau = \pm 2$ have two sides and no corners, since the sides end at the fixed point. See Figure 5.1.

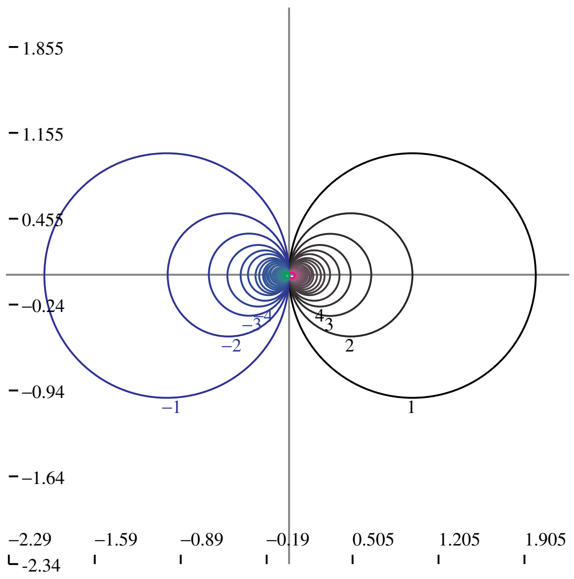

Figure 5.1. Ford and Dirichlet domains for parabolic elements

5.2. **Elliptic generators.** Consider elliptic elements of the form (2.5). Using formulæ (3.3) and (3.5), some tedious algebra yields that the center and radius of both the equidistant and isometric hemispheres (if $\rho > 0$) are given by

$$\begin{array}{rcl} C_n & = & \frac{1}{2} - i\frac{\cot n\theta}{2} \quad \text{and} \\ R_n & = & \left|\frac{\csc n\theta}{2}\right| \end{array} \tag{5.1}$$

and all pass through the fixed points 0 and 1. If the generator is of infinite order, then Γ does not act properly discontinuously on any subset of $\widehat{\mathbb{C}}$ and there is no Ford or Dirichlet domain. There is also no Dirichlet fundamental domain when $\rho = 0$, since the proposed center of the domain is a fixed point.

If the generator is of finite order, then $\theta = \pi\frac{k}{\ell}$ where k and $\ell \neq \pm 1$ are relatively prime integers. The largest imaginary part of any point on the circle $\widehat{X}_n$ is

$$f(\psi) = \frac{1}{2}\left(|\csc\psi| - \cot\psi\right)$$

and the smallest such imaginary part is

$$g(\psi) = -\frac{1}{2}\left(|\csc\psi| + \cot\psi\right),$$

where $\psi = \frac{nk}{\ell}$. As a function of $\psi \in (0, \pi)$, f is positive and strictly decreasing, while for general ψ it is periodic with period π. It follows that the arc of $\widehat{X}_n$ from 0 to 1 and above the x-axis will form one of the sides of our fundamental domain if n is an integer for which nk is the smallest possible non-zero value modulo ℓ, *i.e.*, if $nk \cong 1 \mod \ell$; the most appropriate label to use for this side, among the infinitely many solutions of this equation, is the one of smallest absolute value. By symmetry or similar reasoning with $g(\psi) = -f(-\psi)$, the other side of the fundamental domain will be the corresponding piece of $\widehat{X}_{-n}$. The fixed points 0 and 1 are the endpoints of the sides. See Figure 5.2 for an example.

5.3. **Loxodromic generators.** For this subsection, ρ shall be a fixed non-negative real number or ∞, where in the former case we work with Dirichlet domains and our favorite basepoint (3.2) and in the latter we work with Ford domains. The method we shall employ for loxodromic γ is to see how the combinatorial type of the fundamental domain $\widehat{\Delta}$ changes with continuous deformations of the trace τ. Fundamental to the success of this approach is the continuity of the centers and radii of the isometric and equidistant circles with respect to τ, as described in Proposition 3.1.

To begin, note that if τ is purely imaginary and of modulus greater than 2, then direct (if long) calculation with (3.3) and (3.5) yields that all the $\widehat{X}_i$ are disjoint. Hence $\widehat{\Delta}$ is bounded by the non-intersecting sides $S_1 = \widehat{X}_1$ and $S_{-1} = \widehat{X}_{-1}$; see Figure 5.3 for an example with $\tau = 3i$ and $\rho = 1$.

If we now vary τ, the first change in the combinatorial type of $\widehat{\Delta}$ can only occur when some $\widehat{X}_{\pm m}$ becomes internally tangent to $\widehat{X}_{\pm 1}$ or when $\widehat{X}_{-1}$ becomes externally tangent to $\widehat{X}_1$ at some point q. By Proposition 4.7, these two possibilities are actually the same, and happen only if $m = 2$ and $q = \frac{1}{2}$. In fact, Proposition 4.3 tells us that $\widehat{X}_1$ passes through $\frac{1}{2}$ if and only if it is tangent to $\widehat{X}_{-1}$ there; let us define Σ_ρ to be the set of traces τ for which this happens. There are two cases, different only in the algebra.

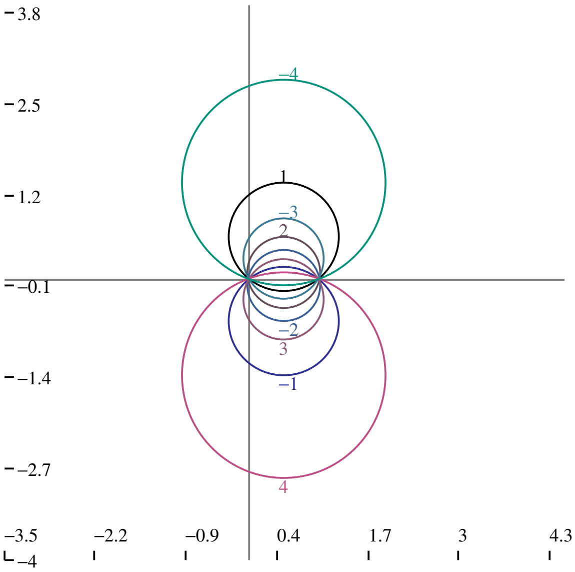

FIGURE 5.2. Ford and Dirichlet domain for elliptic element of trace $2\cos\frac{2\pi}{9}$

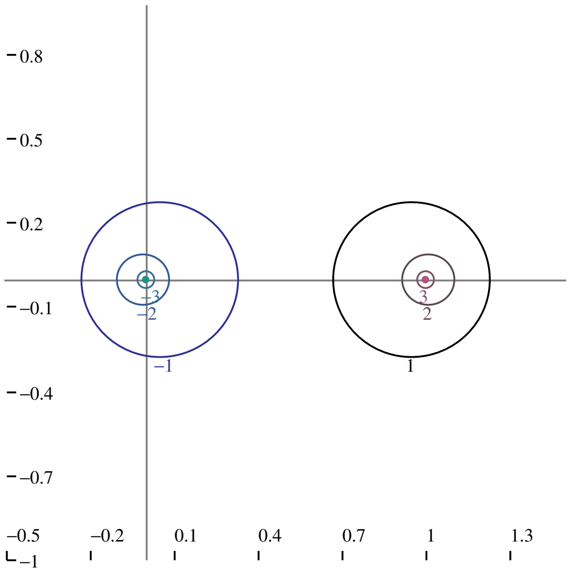

FIGURE 5.3. Dirichlet domain with $\tau = 3i$ and $\rho = 1$

- Σ_∞ is the circle $|\tau| = 2$. See Figure 5.4 for an example of a Ford domain for a generator with trace outside of Σ_∞.
- For $\rho < \infty$, Σ_ρ is a convex curve lying inside of Σ_∞ and touching it at $\tau = \pm 1$. For an example of a Dirichlet domain with basepoint at distance 1 from the axis for a generator with trace outside of Σ_1 (but inside Σ_∞) see Figure 5.5.

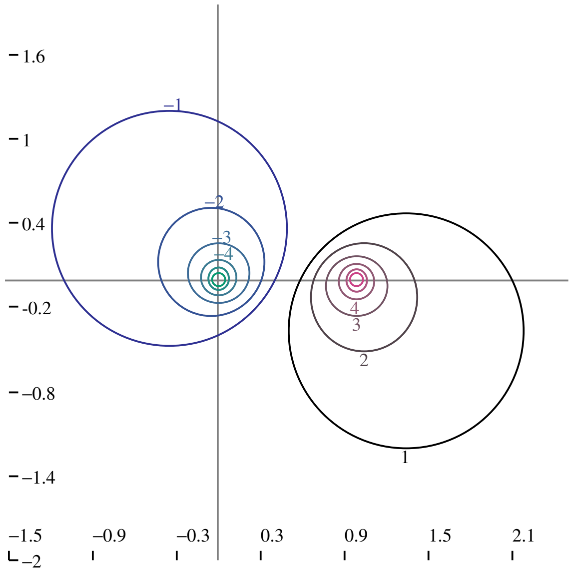

FIGURE 5.4. Ford domain for an element with $|\tau| > 2$

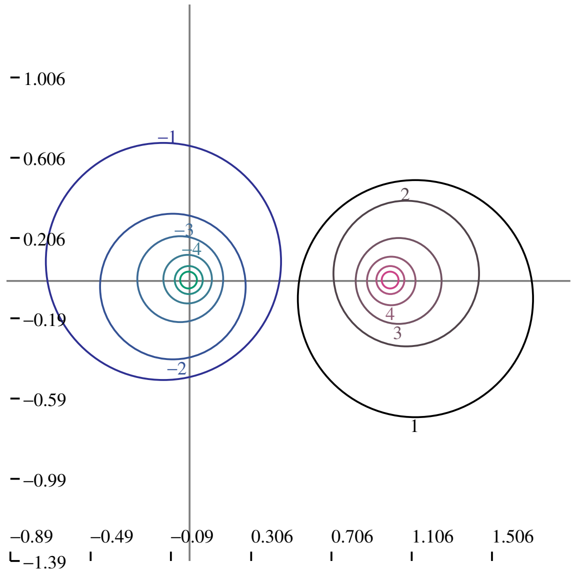

FIGURE 5.5. Dirichlet domain based at distance 1 from the axis for an element with $\tau = 1 + i$

In both cases, the fundamental domain has $\widehat{X}_{\pm 1}$ as its two disjoint sides if and only if τ is outside Σ_ρ; for traces inside Σ_ρ, $\frac{1}{2}$ sits inside both $\widehat{X}_1$ and $\widehat{X}_{-1}$. Figure 5.6 shows some sample curves Σ_ρ.

For the remainder of this subsection, we focus on the combinatorial type of both the Ford and Dirichlet domains on $\widehat{\mathbb{C}}$. When τ is on Σ_ρ, the fundamental domain

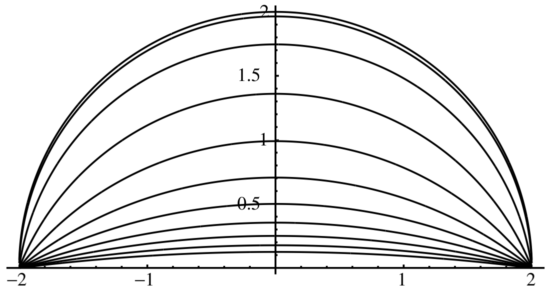

FIGURE 5.6. Curves Σ_ρ in the upper half-plane for $\rho = 2^j$, $-8 \leq j \leq 2$, $j \in \mathbb{Z}$

$\widehat{\Delta}$ is bounded by the two sides $\widehat{X}_1$ and $\widehat{X}_{-1}$ which intersect at the point $\frac{1}{2}$. In fact, to be completely precise, we should say that fundamental domains with $\tau \in \Sigma_\rho$ have four sides, where each side is thought of as a part of $\widehat{X}_{\pm 1}$ whose endpoints are the points of external and internal tangency. Points of internal tangency certainly exist, as $\widehat{X}_{\pm 2}$ is internally tangent to $\widehat{X}_{\pm 1}$ by Proposition 4.7. See Figure 5.7 for an example.

Let B_ρ be the interior of Σ_ρ in the upper half τ-plane minus the real axis. As was noted above, for $\tau \in B_\rho$, $\widehat{X}_1$ and $\widehat{X}_{-1}$ intersect. Since all positive isometric or equidistant circles intersect at 1, as do all the negative ones at 0, it follows that the complement of the fundamental domain is connected if and only $\tau \in B_\rho \cup \Sigma_\rho$.

Further, all external tangencies must occur at $\frac{1}{2}$ by Proposition 4.7, so there are no external tangencies for $\tau \in B_\rho$. For some value $\tau^* \in B_\rho$ on the positive imaginary axis both $\widehat{\Delta}$ and its boundary are connected; see Figure 5.8 for B_∞, where $\tau^* = i$ works. Consider continuous paths starting at τ^* and remaining inside B_ρ. Since the complement of $\widehat{\Delta}$ is connected, the only way for $\widehat{\Delta}$ or its boundary to become disconnected along this path is for two sides to become externally tangent, which is impossible. We have thus established

Lemma 5.3. *For every $\tau \in B_\rho$, the fundamental domain $\widehat{\Delta}$, its complement and its boundary are all connected.*

We may describe $\partial\widehat{\Delta}$, uniquely up to cyclic permutation, by the counterclockwise sequence of (components of) sides

$$S_{n_0}, \ldots, S_{n_{k-1}},$$

such that every adjacent pair of (components of) sides meet at a corner, including $S_{n_{k-1}}$ and S_{n_0}. It often happens that k is six, in which case there is a relation among the indices of the sides that can appear.

Lemma 5.4. *If $\widehat{\Delta}$ is a connected six-sided domain (or a four-sided domain for which two sides have two connected components), then the side sequence of $\widehat{\Delta}$ is in fact*

$$S_n, S_{n+m}, S_m, S_{-n}, S_{-m-n}, S_{-m}. \tag{5.2}$$

Proof. We begin by writing the sides of $\widehat{\Delta}$ as

$$S_{n_0}, S_{n_1}, S_{n_2}, S_{n_3}, S_{n_4}, S_{n_5}. \tag{5.3}$$

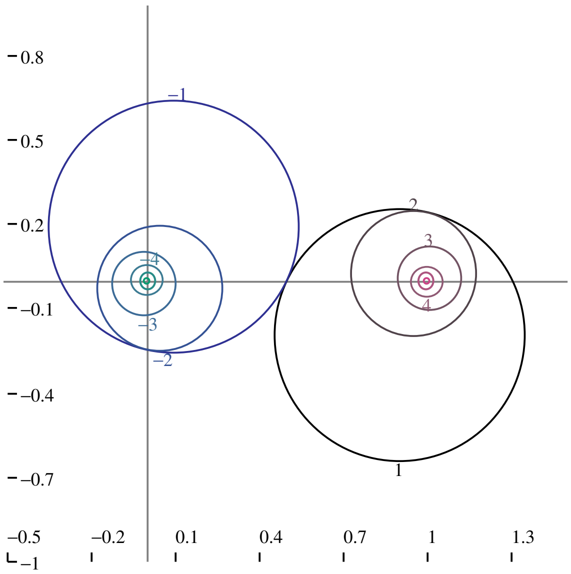

FIGURE 5.7. Ford domain for an element with $|\tau| = 2$

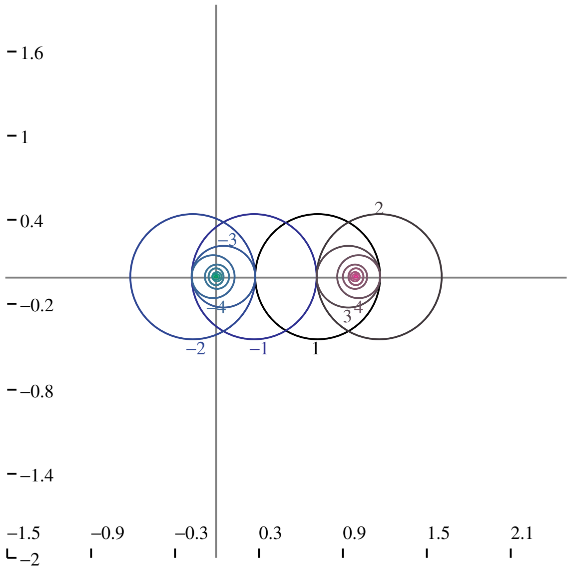

FIGURE 5.8. Ford domain for an element with $\tau = i$

The existence of the diffeomorphism ϕ in Proposition 4.3 implies that $n_i = -n_{i+3}$; here and for the rest of this proof, arithmetic with the subscript i shall always be modulo six. Indexing the corners of $\widehat{\Delta}$ as

$$c_i = S_{n_i} \cap S_{n_{i+1}},$$

Proposition 4.2 tells us that $\gamma^{-n_i}\, c_i = c_{i+2}$. But now, following Figure 5.9,

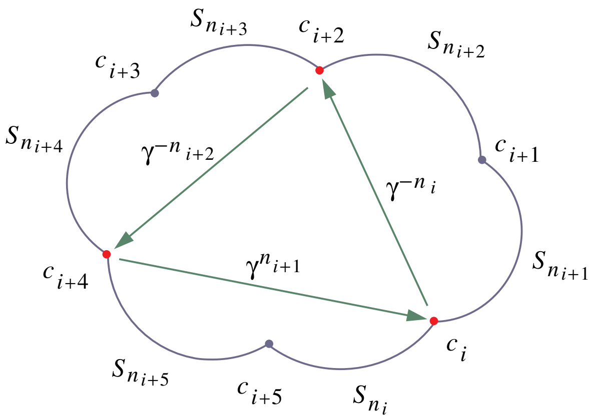

FIGURE 5.9. Moving around the corners of a six-sided domain on $\partial\mathbb{H}^3_{\mathbb{R}}$

$$c_i = \gamma^{-n_{i+4}}\, c_{i+4} = \gamma^{n_{i+1}}\, c_{i+4} = \gamma^{n_{i+1}-n_{i+2}}\, c_{i+2} = \gamma^{n_{i+1}-n_{i+2}-n_i}\, c_i.$$

Since corners cannot be fixed points for non-identity group elements we must have

$$n_{i+1} - n_{i+2} - n_i = 0,$$

hence we can rewrite (5.3) as (5.2). □

The above proposition can be directly verified for the Ford domain when $\tau = i$, where the side sequence is

$$S_1, S_2, S_1, S_{-1}, S_{-2}, S_{-1};$$

see Figure 5.8.

A similarly nice situation occurs when there are four sides.

Lemma 5.5. *If $\widehat{\Delta}$ has four connected sides, then the side sequence of $\widehat{\Delta}$ is*

$$S_n, S_m, S_{-n}, S_{-m}. \tag{5.4}$$

Moreover, the corner at the intersection of S_i and S_j also lies on $\widehat{X}_{i+j}$.

Proof. Represent $\widehat{\Delta}$ by the side sequence

$$S_{n_0}, S_{n_1}, S_{n_2}, S_{n_3}.$$

As above, the existence of the diffeomorphism ϕ in Proposition 4.3 implies that $n_i = -n_{i+2}$, where for the present proof arithmetic with the subscript i is to be taken modulo four. Labeling each corner $c_i = S_{n_i} \cap S_{n_{i+1}}$ we now have $\gamma^{-n_i}\, c_i = c_{i+1}$. Hence $\gamma^{-n_{i+1}-n_i}\, c_i = c_{i+2}$ (see Figure 5.10), so by Proposition 4.1, $\widehat{X}_{n_i+n_{i+1}}$ intersects $\partial\widehat{\Delta}$ at the corner c_i where the sides S_{n_i} and $S_{n_{i+1}}$ meet. □

An example of a Ford domain with four sides, corresponding to trace $.6\overline{3} + .9\overline{3}i$, appears in Figure 5.11.

We are now ready to prove the following central result.

Theorem 5.6. *For every $\tau \in B_\rho$, $\partial\widehat{\Delta}$ has four or six sides.*

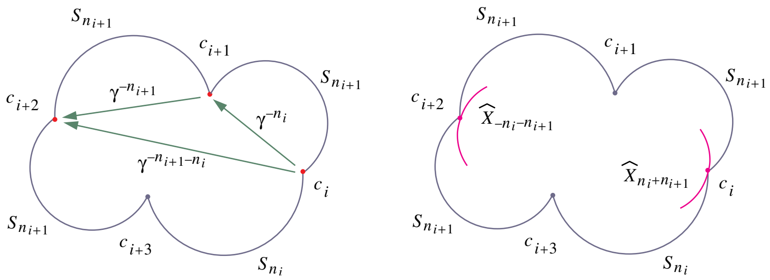

FIGURE 5.10. Moving around the corners of a four-sided domain on $\partial\mathbb{H}^3_{\mathbb{R}}$

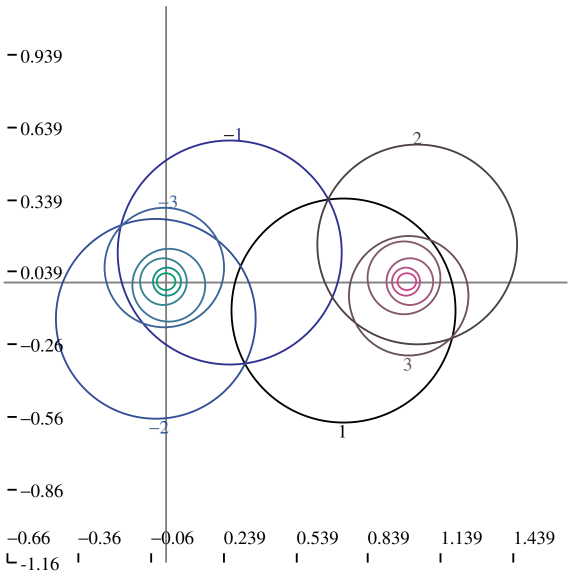

FIGURE 5.11. A four-sided Ford domain

Proof. What is left to prove is that for a four- or six-sided $\widehat{\Delta}$ if τ is varied continuously in B_ρ, then $\widehat{\Delta}$ for the new τ can have only four or six sides – two-sided domains must have sides $S_{\pm 1}$ and these occur only on Σ_ρ. Note that by Proposition 4.7, new sides can only appear from the vertices, so we shall concentrate our attention there.

Case I: $\widehat{\Delta}$ *has four connected sides.* In Lemma 5.5 we have enumerated the $\widehat{X}_n$'s which are incident to the corners of $\widehat{\Delta}$, and by Proposition 4.4 these are the only ones possible. For a sufficiently small change in τ, then, we would either continue to have a four-sided domain with the same sides as $\widehat{\Delta}$, two of the four curves $\widehat{X}_{\pm n \pm m}$ known to pass through the corners would contribute actual sides to $\widehat{\Delta}$, or all four of these curves would. It is this last case which we must exclude.

The side sequence in question is

$$S_n, S_{n+m}, S_m, S_{m-n}, S_{-n}, S_{-n-m}, S_{-m}, S_{n-m}.$$

If we write $c_{i,j}$ for the corner formed by the sides S_i and S_j, then

$$\begin{aligned} c_{n,n+m} &= \gamma^m \gamma^{n-m} \gamma^{-n} c_{n,n+m} = \gamma^m \gamma^{n-m} c_{m-n,-n} \\ &= \gamma^m c_{-m,n-m} = c_{n+m,m} ; \end{aligned}$$

see Figure 5.12. But $c_{n,n+m} \neq c_{n+m,m}$, ruling out this possibility.

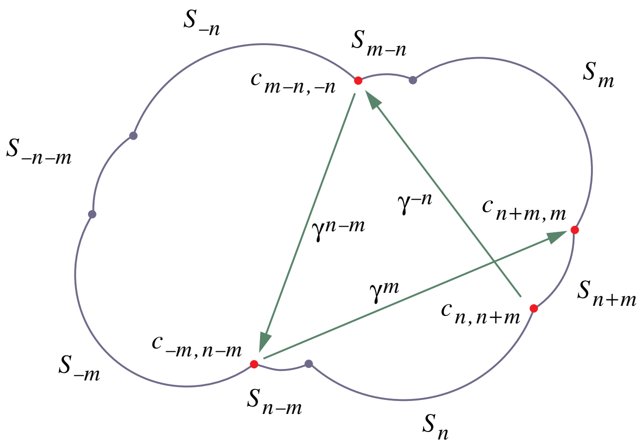

FIGURE 5.12. An impossible picture for *Case* I of Theorem 5.6

Case II: *$\widehat{\Delta}$ has six connected sides or four sides, two of which have two components.* We shall show that in this case no $\widehat{X}_k$ can be incident to any corner of $\widehat{\Delta}$, so that in fact the domains with the same side configuration as $\widehat{\Delta}$ correspond to an open set of traces in B_ρ. Thus small deformations of τ in this set do not increase the number of sides.

Assume on the contrary that some $\widehat{X}_k$ is incident to the corner $c_{n,n+m}$, where we label corners as in the previous case. By symmetry, $\widehat{X}_{-k}$ must be incident to $c_{-n,-n-m}$. Now, as is illustrated in Figure 5.13,

$$\gamma^{n-k} c_{n,n+m} = \gamma^n \gamma^{-k} c_{n,n+m} = \gamma^n c_{-n,-n-m} = c_{-m,n} .$$

By Proposition 4.1, $\widehat{X}_{k-n}$ contributes to $\partial\widehat{\Delta}$ by at least the point $c_{n,n+m}$ and $\widehat{X}_{n-k}$ by the point $c_{-m,n}$. However, if $\widehat{X}^{\partial}_{k-n} = c_{n,n+m}$, then Proposition 4.4 would tell us that $k-n=k$, which is impossible. Thus $k-n$ must instead equal n or $n+m$, as these are the indices of the sides incident to $c_{n,n+m}$.

Sub-case IIa: $k-n=n$. Thus $k=2n$, so

$$\gamma^{m-n} c_{n,n+m} = \gamma^{n+m} \gamma^{-2n} c_{n,n+m} = \gamma^{n+m} c_{-n,-n-m} = c_{n+m,m} ,$$

see Figure 5.14.

By the same analysis as above, it follows that $c_{n,n+m} \in \widehat{X}_{n-m}$ and $n-m$ must equal $2n$, n or $n+m$. But this would imply that m is equal to $-n$ or 0, which it is not, so this sub-case is excluded.

Sub-case IIb: $k-n=n+m$. Here $k=2n+m$ and our contradiction is

$$\begin{aligned} c_{m,-n} &= \gamma^{n+m} \gamma^{-2n-m} \gamma^n c_{m,-n} = \gamma^{n+m} \gamma^{-2n-m} c_{n,n+m} \\ &= \gamma^{n+m} c_{-n,-n-m} = c_{n+m,m} , \end{aligned}$$

following Figure 5.15. $\square$

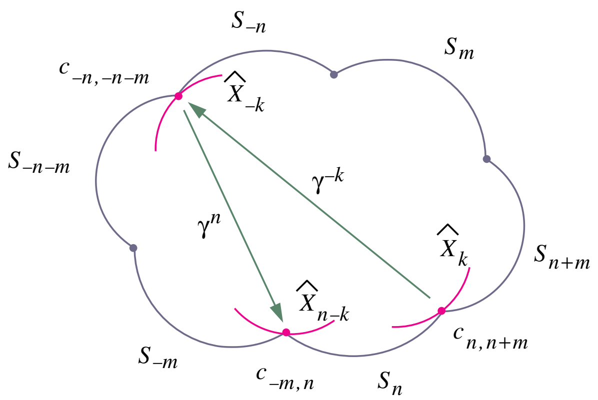

FIGURE 5.13. *Case* II of Theorem 5.6

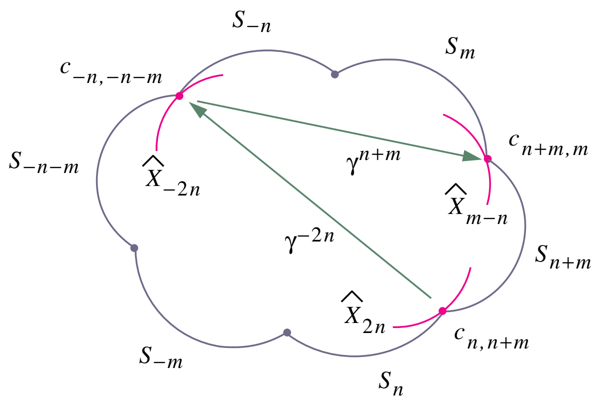

FIGURE 5.14. *Sub-case* IIa of Theorem 5.6, $k = 2n$

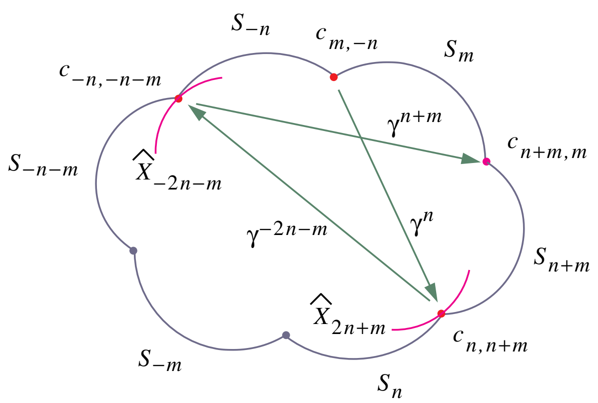

FIGURE 5.15. *Sub-case* IIb of Theorem 5.6, $k = 2n + m$

Note that Lemma 5.5, Theorem 5.6 and the proof its *Case* II easily give the following statement, which will be useful later:

Corollary 5.7. *With a loxodromic generator γ, the only situation in which some $\widehat{X}_n$ touches $\partial\widehat{\Delta}$ from the inside at a corner between sides S_j and S_k is when the domain has four sides and $n = j + k$.*

6. The decomposition of the trace plane

In this section, we give a complete decomposition of the trace plane into regions for which the associated fundamental domain is of fixed combinatorial type. We have seen in the previous section that these combinatorial types have very limited possibilities.

Definition 6.1. A fundamental domain $\widehat{\Delta}$ or the trace to which it corresponds to will be said to be

- *of type* $\{n, n+m, m\}$ if $\widehat{\Delta}$ has a six-sided boundary as in (5.2) with $n, m > 0$;
- *of type* $\{n, m\}$ if $\widehat{\Delta}$ has a four-sided boundary as in (5.4) with $n, m > 0$; and
- *of type* $\{n\}$ if the boundary of $\widehat{\Delta}$ consists exactly of the sides $S_{\pm n}$.

The sets of traces in $\mathcal{U}$ of these types will be denoted $\mathcal{S}_{\{n,n+m,m\}}$, $\mathcal{F}_{\{n,m\}}$ and $\mathcal{T}_{\{n\}}$, respectively (for "six-sided", "four-sided", *etc.*).

We have seen in the proof of Theorem 5.6 that the set $\mathcal{S}_{\{n,n+m,m\}}$ is open in $\mathcal{U}$, while $\mathcal{F}_{\{n,m\}}$ is closed and in fact a real algebraic curve. This is because the traces of type $\{n, m\}$ are exactly those for which $\widehat{X}_n$, $\widehat{X}_{n+m}$ and $\widehat{X}_m$ meet at one point on the boundary of $\widehat{\Delta}$. For example, $\mathcal{F}_{\{1,1\}}$ is exactly the curve Σ_ρ used in §5.

Domains of type $\{n\}$ come from three different situations. One is due to elliptic elements with traces in the real segment $(-2, 2)$; here all n occur and the sides $S_{\pm n}$ intersect at the points 0 and 1. Another comes from hyperbolic elements, *i.e.*, with real traces of absolute value greater than 2; these have fundamental domains with disjoint sides $S_{\pm 1}$. The last corresponds to the open set of traces in $\mathcal{U}$ exterior to Σ_ρ for which the fundamental domain again has disjoint sides $S_{\pm 1}$.

Next we mention two elementary symmetries that the decomposition of $\mathcal{U}$ must exhibit. The first stems from the fact that elements of $PSL_2(\mathbb{C})$ are only defined up to scalar multiplication by ± 1, so traces are only defined up to multiplication by ± 1. We thus can and do restrict our attention to traces with non-negative imaginary parts, *i.e.*, we shall decompose $\mathcal{U} \cup \mathbb{R}$, rather than the entire complex plane of traces.

The other symmetry of the trace plane arises from complex conjugation $z \mapsto \overline{z}$ on $\widehat{\mathbb{C}}$, which extends to an isometry of $\mathbb{H}^3$ reflecting in the vertical plane containing the real axis. Conjugation of an element $\gamma \in PSL_2(\mathbb{C})$ by this isometry results in an isometry $\gamma' \in PSL_2(\mathbb{C})$ of $\mathbb{H}^3$ whose trace is the complex conjugate of the trace of γ. The domains corresponding to γ' will be reflections through the vertical plane containing the real axis of the corresponding domains of γ.

Applying both of the above symmetries, we see that reflection of the trace plane across the imaginary axis takes any $\mathcal{S}_{\{n,n+m,m\}}$ to $\mathcal{S}_{\{m,m+n,n\}}$, $\mathcal{F}_{\{n,m\}}$ to $\mathcal{F}_{\{m,n\}}$ and $\mathcal{T}_{\{n\}}$ to itself.

6.1. Deformations, again.

Let us now examine, once again, how small changes in the trace can affect the picture we are studying. First, the proof of Theorem 5.6 can be squeezed for yet more information:

Proposition 6.2. *Let n and m be relatively prime, positive integers.*

- *Limit points in $\mathcal{U}$ of sequences in $\mathcal{S}_{\{n,n+m,m\}}$ can only lie on $\mathcal{F}_{\{n,m\}}$, $\mathcal{F}_{\{n,n+m\}}$ or $\mathcal{F}_{\{n+m,m\}}$.*
- *Points in $\mathcal{F}_{\{n,m\}}$ can only lie in the closure of $\mathcal{S}_{\{n,n+m,m\}}$ or*
  - *$\mathcal{S}_{\{n-m,n,m\}}$ if $n > m$,*
  - *$\mathcal{S}_{\{n,m,m-n\}}$ if $m > n$, or*
  - *$\mathcal{T}_{\{1\}}$ if $n = m = 1$.*

This immediately has one useful consequence. Imagine filling up $\mathcal{U}$ with the sets $\mathcal{S}_{\{n,n+m,m\}}$ and $\mathcal{F}_{\{n,m\}}$. If n and m are relatively prime, then $n+m$ is relatively prime to both n and m. Because 1 is relatively prime to itself and the above permitted adjacencies take relatively prime n and m to new relatively prime pairs, by induction we have

Corollary 6.3. *If $\mathcal{S}_{\{n,n+m,m\}}$ or $\mathcal{F}_{\{n,m\}}$ is a type of fundamental domain which actually occurs for some traces in $\mathcal{U}$, then n and m are relatively prime.*

These general restrictions on the change of domain type under limits of traces are, however, not enough to finish the task of determining the decomposition of the trace plane. For a more precise result, we must consider what happens in the neighborhood of a point $\tau_0 \in \mathcal{F}_{\{n,m\}}$. In particular, consider the curve of traces given by $t \mapsto \tau_t = \tau_0 + it$ for $t \in (-\epsilon, \epsilon)$. Plugging τ_t into (2.9) we can then use (3.5) and (3.3) to determine the isometric and equidistant circles. When $t = 0$, $\widehat{X}_n$ and $\widehat{X}_m$ intersect and the point of intersection lies on $\widehat{X}_{n+m}$; a very direct if very tedious calculus exercise shows that the intersection point is outside $\widehat{X}_{n+m}$ for sufficiently small $t > 0$ and inside for sufficiently small $t < 0$. This gives us the information we needed and is worth stating in the form we shall later use.

Proposition 6.4. *Directly below any point in the trace plane $\mathcal{U}$ which lies on the curve $\mathcal{F}_{\{n,m\}}$ are points of $\mathcal{S}_{\{n,n+m,m\}}$, while directly above are points of $\mathcal{S}_{\{n-m,n,m\}}$ if $n > m$, $\mathcal{S}_{\{n,m,m-n\}}$ if $m > n$ or $\mathcal{T}_{\{1\}}$ if $n = m = 1$.*

6.2. **Near the real axis.** In this subsection we shall examine the consequences for the trace plane decomposition of the geometric continuity up to the boundary of $\mathcal{U}$ described in §3.3. We start with some set $\mathcal{A}$ of traces of a fixed type, either $\mathcal{A} = \mathcal{S}_{\{n,n+m,m\}}$ or $\mathcal{A} = \mathcal{F}_{\{n,m\}}$, and see what limit points $\mathcal{A}$ may have on the real axis. So let $t \mapsto \tau_t$ for $0 \le t \le 1$ be a continuous curve which lies in $\mathcal{A}$ for $0 \le t < 1$ and for which τ_1 lies on the real segment $[-2, 2]$, let γ_t be the generator corresponding to τ_t by (2.9) and (2.7), and let $\widehat{X}_{k,t}$ denote the corresponding equidistant or isometric circles.

Suppose that τ_1 corresponds to an irrational rotation. Then no power of γ_1 is the identity, so all circles $\widehat{X}_{k,t}$ are well-defined – but powers of γ_1 get arbitrarily close to the identity, so there are $\widehat{X}_{k,1}$ of arbitrarily large radius. Let

$$M = \sup_{t\in[0,1]} \left\{ \text{radius of } \widehat{X}_{j,t} \mid j \in \{n, m, n+m\} \right\}.$$

(Here, if $\mathcal{A}$ is a region of type $\mathcal{F}_{\{n,m\}}$ for $t < 1$, then $j = n + m$ is superfluous but causes no problems.) As noted above, we can find an exponent k such that the radius of $\widehat{X}_{k,1}$ is much larger than M. By continuity, there exists a $t_b \in [0, 1)$ such that the radius of $\widehat{X}_{k,t_b}$ is also much larger than M, say at least $2M + 1$. But then $\widehat{X}_{k,t_b}$ could not possibly lie completely in the interior of the circles $\widehat{X}_{\pm n,t_b}$, $\widehat{X}_{\pm m,t_b}$

and $\widehat{X}_{\pm(n+m),t_b}$. This is a contradiction to the assumption that $\tau_{t_b} \in \mathcal{A}$, so τ_1 must be rational.

Now let $\tau_1 = 2\cos\frac{p\pi}{q}$ where p and q are relatively prime positive integers and $0 \leq p < q$. Since γ_1 is of order q, as $t \to 1$ the corresponding $\widehat{X}_q$ has radius going to infinity; we claim that in fact $\widehat{X}_q$ provides one of the sides of the fundamental domains of type $\mathcal{A}$. At least one of the sides must have a radius which is also going to infinity and so must be labeled by a multiple kq of q. For $\gamma'_t = \gamma_t^q$, it would suffice to show that for γ' very close to Id the circle $\widehat{X}'_1$ is much larger than $\widehat{X}'_k$. If γ' is elliptic and extremely close to Id, then this is the case, since by Proposition 3.1 all $\widehat{X}'_j$ will be defined up to $j \gg k$ and by (5.1)

$$R'_j = \left|\frac{\csc j\theta}{2}\right| \approx \left|\frac{1}{2j\theta}\right|.$$

But as $\gamma' \to \mathrm{Id}$ in $\mathcal{U}$ it is always nearer and nearer the elliptic elements we have just described, so the continuity of R_n tells us that $\widehat{X}'_1 = \widehat{X}_q$ must always contribute a side to the fundamental domain.

Thus we have shown that

Proposition 6.5. *Limit points of* $\mathcal{S}_{\{n,n+m,m\}}$ *(respectively,* $\mathcal{F}_{\{n,m\}}$*) on* $[-2,2]$ *are* $2\cos\frac{p}{q}\pi$ *where* p *and* q *are relatively prime and* $q \in \{n, m, n+m\}$ *(respectively,* $q \in \{n,m\}$*).*

6.3. **Farey sequences.** Before finishing the decomposition of the trace plane, we recall some elementary number theory (see [3] for an exposition).

Definition 6.6. The *Farey sequence of order* i (between 0 and 1) is the sequence of reduced fractions with denominators not exceeding i, listed in increasing order.

The Farey sequence of order i is also given by the i^{th} row of the following construction:

$$\begin{array}{ccccccc}
\frac{0}{1} & & & & & & \frac{1}{1} \\
\frac{0}{1} & & & \frac{1}{2} & & & \frac{1}{1} \\
\frac{0}{1} & & \frac{1}{3} & \frac{1}{2} & \frac{2}{3} & & \frac{1}{1} \\
\frac{0}{1} & \frac{1}{4} & \frac{1}{3} & \frac{1}{2} & \frac{2}{3} & \frac{3}{4} & \frac{1}{1}
\end{array}$$

Here the i^{th} row, for $i > 1$, is composed of the $(i-1)^{\text{st}}$ with the insertion of all the numbers $\frac{p+q}{n+m}$ between consecutive fractions $\frac{p}{n} < \frac{q}{m}$ in the $(i-1)^{\text{st}}$ row, provided that $n + m \leq i$.

This sequence has many nice properties, including the following:

- each fraction (except $\frac{0}{1}$ and $\frac{1}{1}$) is written in reduced form;
- the fraction $\frac{p+q}{n+m}$ between consecutive elements $\frac{p}{n}$ and $\frac{q}{m}$ in the Farey sequence of some order is the unique reduced fraction with denominator $n+m$ between $\frac{p}{n}$ and $\frac{q}{m}$;
- for each relatively prime n and m, there exist unique reduced fractions $\frac{p}{n} < \frac{q}{m}$ occurring consecutively in the Farey sequence of some order. (Exercise 5 on page 301 of [3] is to show existence and uniqueness is also an easy exercise.)

Starting with a relatively prime n and m and the unique reduced fractions $\frac{p}{n} < \frac{q}{m}$ occurring consecutively in the Farey sequence of order i, we can retrace our steps back through the Farey sequences of smaller orders. There exist $\frac{p_j}{n_j}$ and $\frac{q_j}{m_j}$

occurring consecutively in the Farey sequence of order $i-j$, for $0 \leq j \leq i-1$, such that

$$\frac{p_j}{n_j} \leq \cdots \leq \frac{p_0}{n_0} = \frac{p}{n} < \frac{q}{m} = \frac{q_0}{m_0} \leq \cdots \leq \frac{q_j}{m_j}.$$

The denominators of these fractions will be seen below to have a special relationship with the faces on the Ford and Dirichlet domains inside hyperbolic space, so we make the

Definition 6.7. The sequence

$$\{n, m\} = \{n_0, m_0\}, \{n_1, m_1\}, \ldots, \{n_k, m_k\} = \{1, 1\}$$

of ordered pairs of denominators of the above fractions with repeated pairs removed, shall be called the *Farey denominator sequence of* $\{n, m\}$.

6.4. **The decomposition.** We are now ready to give the decomposition of the trace plane by types of the corresponding fundamental domains. Let us first discard one trivial case, that of a Dirichlet domain with axis distance $\rho = 0$. These domains, for any loxodromic generator, are of type $\mathcal{T}_{\{1\}}$ with disjoint sides $S_{\pm 1}$; for an elliptic generator, these domains are not defined at all since the basepoint is a fixed point of Γ.

Fix $\rho > 0$ for the remainder of this section. By Theorem 5.2, we know that the trace plane $\mathcal{U}$ is the union of $\mathcal{T}_1$ and all of the regions $\mathcal{F}_{\{n,m\}}$ and $\mathcal{S}_{\{n,n+m,m\}}$ where n and m are relatively prime. We now give a more precise decomposition of $\mathcal{U}$.

Theorem 6.8. *For every positive, relatively prime pair $\{n, m\}$ let $\frac{p}{n} < \frac{q}{m}$ be the unique fractions occurring consecutively in the Farey sequence of some order.*

- *The set $\mathcal{F}_{\{n,m\}}$ is a real algebraic curve which intersects every vertical line in $\mathcal{U}$ at most once and which has limit points $2\cos\frac{p}{n}\pi$ and $2\cos\frac{q}{m}\pi$ on the real axis.*
- *The set $\mathcal{S}_{\{n,n+m,m\}}$ is an open curvilinear triangle bounded above by $\mathcal{F}_{\{n,m\}}$ and below by $\mathcal{F}_{\{n,n+m\}}$ and $\mathcal{F}_{\{n+m,m\}}$; its limit points on the real axis are $2\cos\frac{p}{n}\pi$, $2\cos\frac{p+q}{n+m}\pi$ and $2\cos\frac{q}{m}\pi$.*

Proof. That $\mathcal{F}_{\{n,m\}}$ is a real algebraic curve which intersects every vertical line in $\mathcal{U}$ at most once is a consequence of the definition of $\mathcal{F}_{\{n,m\}}$ and Proposition 6.4.

We know that $\mathcal{T}_{\{1\}}$ consists of the real intervals $(-\infty, 2] \cup [2, \infty)$ together with the part of $\mathcal{U}$ exterior to $\Sigma_\rho = \mathcal{F}_{\{1,1\}}$. Adjacent to this open set, we have seen, lies the convex curve $\mathcal{F}_{\{1,1\}}$, touching the real axis at the points ± 2, or $2\cos\frac{0}{1}\pi$ and $2\cos\frac{1}{1}\pi$.

Our strategy at this point is to inductively attach each $\mathcal{S}_{\{n,n+m,m\}}$ and $\mathcal{F}_{\{n,m\}}$ using Propositions 6.4 and 6.5, until we have exhausted the trace plane; this will enable us to determine all of the types which actually occur and how the regions of traces corresponding to each type sit in $\mathcal{U}$.

Below $\mathcal{F}_{\{1,1\}}$ sits the region $\mathcal{S}_{\{1,2,1\}}$. Below $\mathcal{S}_{\{1,2,1\}}$ sits $\mathcal{F}_{\{1,2\}}$ and/or $\mathcal{F}_{\{2,1\}}$. The endpoints $\mathcal{F}_{\{1,2\}}$ are $2\cos\frac{0}{1}\pi = 2$ and some point of the form $2\cos\frac{p}{2}\pi$. Similarly, the endpoints of $\mathcal{F}_{\{2,1\}}$ are $2\cos\frac{1}{1}\pi = -2$ and some point of the form $2\cos\frac{q}{2}\pi$. It is easy to see that $p = q = 1$, and we note that $\frac{0}{1} < \frac{1}{2} < \frac{1}{1}$ is the Farey sequence of order 1.

We now assume for some relatively prime n and m, $\mathcal{F}_{\{n,m\}}$ has limit points $2\cos\frac{p}{n}\pi$ and $2\cos\frac{q}{m}\pi$ where $\frac{p}{n} < \frac{q}{m}$ are the unique fractions occurring consecutively in the Farey sequence of some order i.

$\mathcal{S}_{\{n,n+m,m\}}$ lies below $\mathcal{F}_{\{n,m\}}$, while $\mathcal{F}_{\{n,n+m\}}$ and $\mathcal{F}_{\{n+m,m\}}$ are the possible regions lying below $\mathcal{S}_{\{n,n+m,m\}}$. Both $\mathcal{F}_{\{n,n+m\}}$ and $\mathcal{F}_{\{n+m,m\}}$ must have an endpoint of the form $2\cos\frac{r}{n+m}\pi$, where $\frac{r}{n+m}$ is in reduced form. Since $\frac{p}{n} < \frac{q}{m}$ are fractions occurring consecutively in the Farey sequence of order i, the only fraction in reduced form with denominator $n+m$ between $\frac{p}{n}$ and $\frac{q}{m}$ is $\frac{p+q}{n+m}$. Therefore, $\mathcal{F}_{\{n,n+m\}}$ has endpoints $2\cos\frac{p}{n}\pi$ and $2\cos\frac{p+q}{n+m}\pi$, and $\mathcal{F}_{\{n,n+m\}}$ has endpoints $2\cos\frac{p+q}{n+m}\pi$ and $2\cos\frac{q}{m}\pi$. We note that $\frac{p}{n} < \frac{p+q}{n+m} < \frac{q}{m}$ are consecutive fractions in the Farey sequence of order $i+1$.

For every relatively prime n and m, there exist unique reduced fractions $\frac{p}{n} < \frac{q}{m}$ occurring consecutively in the Farey sequence of some order, so $\mathcal{F}_{\{n,m\}}$ and $\mathcal{S}_{\{n,n+m,m\}}$ must be non-empty. □

A large picture of the decomposition for $\rho = \infty$ appears in Figure 6.1, for $\rho = .25$ in Figure 6.2 and a closeup near $1 \in [-2,2]$ with $\rho = \infty$ in Figure 6.3.

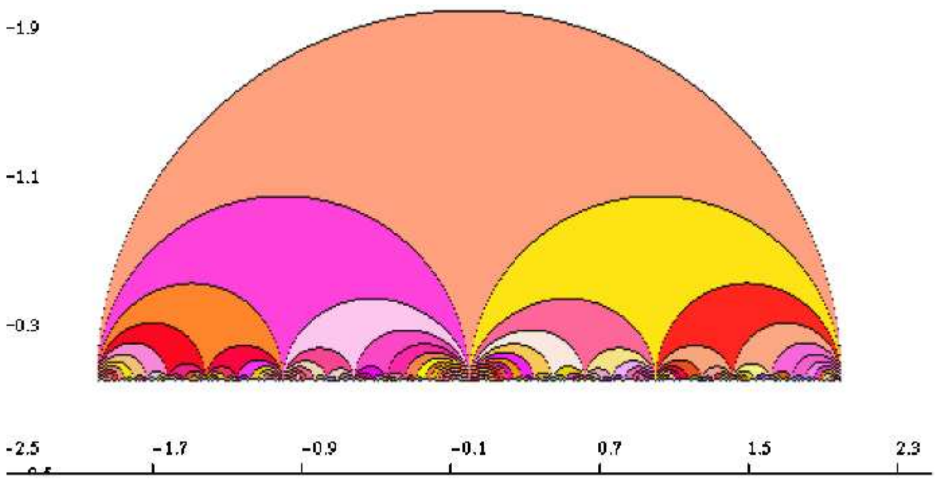

FIGURE 6.1. The decomposition of the trace plane, $\rho = \infty$

We also have the following characterization of the regions which sit above any particular region.

Proposition 6.9. *Let $\{n,m\}$ be a positive, relatively prime pair with corresponding Farey denominator sequence $\{n_0,m_0\},\ldots,\{n_k,m_k\}$. For any $\tau \in \mathcal{S}_{\{n,n+m,m\}}$, the curve $\alpha : [0,2] \to \mathcal{U}$ given by $\alpha(t) = \tau + (2-t)i$ starts in $\mathcal{T}_{\{1\}}$ and then passes successively through each $\mathcal{F}_{\{n_j,m_j\}}$ and then each $\mathcal{S}_{\{n_j,n_j+m_j,m_j\}}$ in turn, as j goes backwards from k to 0, and ends at τ.*

Proof. This is a simple consequence of Propositions 6.2 and 6.4 and the rest of our current discussion. □

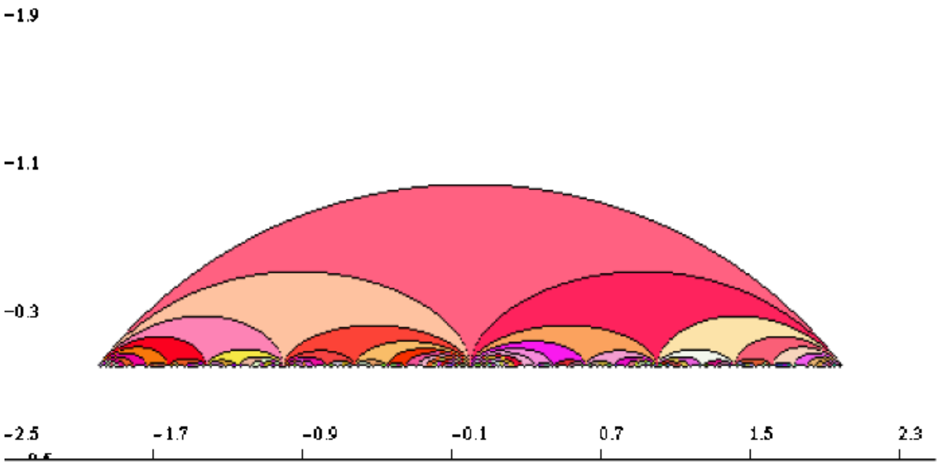

FIGURE 6.2. The decomposition of the trace plane, $\rho = .25$

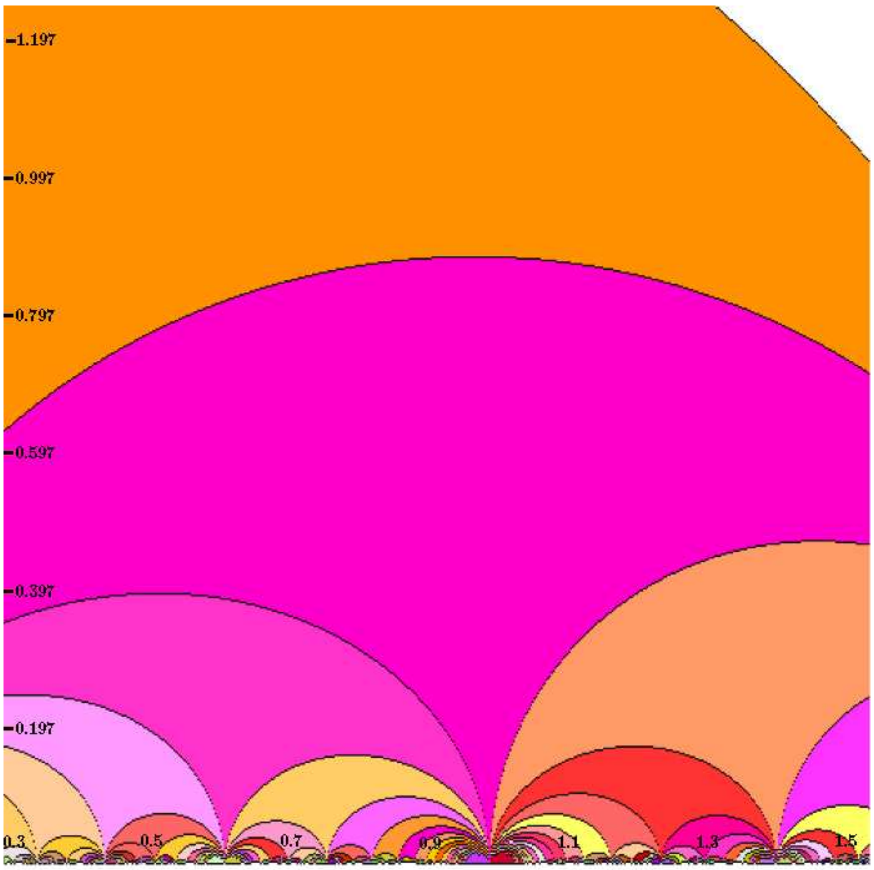

FIGURE 6.3. A closeup near 1 of the decomposition for $\rho = \infty$

7. Fundamental domains inside $\mathbb{H}^3$

The purpose of this section is to extend the techniques and results that we have developed on the boundary of hyperbolic space to its interior, thus giving a complete combinatorial description of the Ford and Dirichlet domains Δ inside $\mathbb{H}^3$ for cyclic loxodromic groups Γ. We shall in fact show that the combinatorial type of $\partial\Delta$ is completely determined by the type of the domain $\widehat{\Delta}$ on $\partial\mathbb{H}^3$, in a way to be explained in detail below.

We start with a simple but useful observation. Suppose Euclidean hemispheres X_n and X_m in $\mathbb{H}^3$ with centers on $\widehat{\mathbb{C}}$ intersect. Their intersection lies in a vertical Euclidean plane $P_{n,m}$ which divides the corresponding half-balls each into two pieces. The part of X_n which is not below X_m is the same as the intersection of X_n with one of the closed half-spaces (half of $\mathbb{H}^3$, that is) bounded by $P_{n,m}$.

A piece X_n^∂ of the boundary of a fundamental domain is the part of X_n which does not lie under any of the other X_m, *i.e.*, it is the intersection of X_n with the half-spaces bounded by the planes $P_{n,m}$ for all other m. Since the intersection of vertical half-spaces is a vertical prism, we have the following

Proposition 7.1. *For any n, the set X_n^∂ on the boundary of a Ford or Dirichlet fundamental domain in $\mathbb{H}^3$ is connected and convex in the hyperbolic sense.*

There is a particular kind of vertex which will occur very frequently in this section, so let us make the

Definition 7.2. A vertex V is called *splendid* if it is in the intersection of the faces F_i, F_j and F_{i+j} and none other.

One reason these vertices are so splendid is given in the following

Proposition 7.3. *If V is a splendid vertex on the faces F_i, F_j and F_{i+j}, then $V = F_i \cap F_j \cap F_{i+j}$ and $\gamma^{i+j}\,\phi(V) = V$.*

Proof. The first statement follows from the fact that the intersection of these faces is a convex set containing the isolated point V. For the second, observe that $\phi(V) \in F_{-i-j}$, so $\gamma^{i+j}\,\phi(V) \in F_{i+j}$. But also

$$\gamma^{-i}\left(\gamma^{i+j}\right)\phi(V) = \gamma^{j}\,\phi(V) \in F_j \subset \partial\Delta$$

since $\phi(V) \in F_{-j}$, so $\gamma^{i+j}\,\phi(V) \in F_i$ by Proposition 4.1; similarly, $\gamma^{i+j}\,\phi(V) \in F_j$. But then $\gamma^{i+j}\,\phi(V) \in F_i \cap F_j \cap F_{i+j} = V$. $\square$

Proposition 7.4. *There can never be a continuous deformation of traces which causes two different splendid vertices on the same edge to coalesce inside $\mathbb{H}^3$.*

Proof. Assume the contrary, so that the vertices $V = F_i \cap F_j \cap F_{i+j}$ and $V' = F_{i'} \cap F_{j'} \cap F_{i'+j'}$ come together in the vertex $W \in \mathbb{H}^3$ by a continuous deformation. By the last Proposition, $\gamma^{-i-j}\,\phi(V) = V$ and $\gamma^{-i'-j'}\,\phi(V') = V'$ all during the deformation, hence also $\gamma^{-i-j}\,\phi(W) = W$ and $\gamma^{-i'-j'}\,\phi(W) = W$. Since loxodromic elements do not have fixed points inside $\mathbb{H}^3$, it follows that $i + j = i' + j'$.

At some point in the deformation sufficiently close to the moment of coalescence, we must have that $F_{i+j} = F_{i'+j'}$ contains both the vertices V and V' and also the edge E connecting them. Relabeling if necessary, we can assume that the other face meeting $F_{i+j} = F_{i'+j'}$ at V and V' and on the other side of E is $F_i = F_{i'}$. Thus, $i = i'$ and $j = j'$. See Figure 7.1.

This contradicts the assumption that V and V' are distinct vertices. $\square$

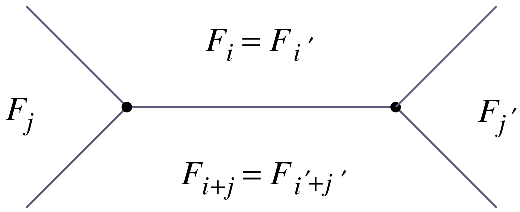

FIGURE 7.1. The impossible coalescence of splendid vertices

Remark 7.5. The figures we will give in this section – such as Figure 7.1 above – depicting configurations of faces, edges and vertices will all be projections of these objects down onto the plane at infinity in our usual half-space model of $\mathbb{H}^3$. It follows that edges will all appear as straight lines connecting either vertices or corners on $\partial\widehat{\Delta}$.

In other words, at least in the restricted situation covered by this Proposition, the combinatorial type of the domain does not change inside $\mathbb{H}^3$ as we vary the trace. This suggests the approach that we shall now follow: we shall demonstrate that the only way faces can appear or disappear on $\partial\Delta$ is along $\partial\widehat{\Delta}$, and these combinatorial additions and subtractions were completely classified in §5.

Let us continue along this path by ruling out various other borderline cases which would have to occur for combinatorial change inside $\mathbb{H}^3$.

Proposition 7.6. *Let V be a splendid vertex of $\partial\Delta$. There can be no hemisphere X_k for which $X_k^\partial = V$.*

Proof. Say $V = F_i \cap F_j \cap F_{i+j}$. By our symmetry Proposition 4.3, $\phi(V) = X_{-k}^\partial$, or $\gamma^k\,\phi(V) = V$. But as this is a splendid vertex, we also have $\gamma^{i+j}\,\phi(V) = V$. Hence $\gamma^{i+j-k}\,V = V$ and so we must have $i + j = k$, since loxodromic elements do not have fixed points inside $\mathbb{H}^3$. □

Next we consider one-dimensional intersections of some hemisphere and the boundary $\partial\Delta$:

Proposition 7.7. *Let E be an edge of $\partial\Delta$ connecting two splendid vertices. Then there can be no hemisphere X_k for which $X_k^\partial = E$.*

Proof. Say one end of E is the vertex $V = F_i \cap F_j \cap F_{i+j}$ and the other end is $W = F_{i'} \cap F_{i'} \cap F_{i'+j'}$. By Proposition 7.3, $\gamma^{-i-j}\,V = \phi(V)$. If $\gamma^{-k}\,V = \phi(V)$, then the same fixed-point argument used in the proof of Proposition 7.6 would imply that $i+j = k$. Thus, X_k^∂ would be a face and not merely an edge. But γ^{-k} takes E to $\phi(E)$ homeomorphically, so the only remaining possibility is that $\gamma^{-k}\,V = \phi(W)$ and $\gamma^{-k}\,W = \phi(V)$.

It is useful to note here that E and $\phi(E)$ are disjoint, by the following series of contradictions. Suppose first that $\phi(E) = E$, so that $\gamma^{-k}\,E = \phi(E) = E$ and γ^{-k} must have a fixed point on $\partial\Delta$, which is impossible. Next, since E and $\phi(E)$ are distinct edges they can only intersect in at most one vertex, say $\phi(V) = W$ (or $\phi(W) = V$). But then $\phi(W) = \phi(\phi(V)) = V$ (respectively, $\phi(V) = \phi(\phi(W)) = W$), so also the other vertex would be a point of intersection. Finally, if ϕ fixes a vertex, then so does γ^{-k}, which is another contradiction.

Now, consider the following calculations, where $r = i + j - k$:

$$\gamma^r W = \gamma^{i+j}(\gamma^{-k} W) = \gamma^{i+j}\,\phi(V) = V,$$

$$\gamma^r \phi(V) = \gamma^{-k}(\gamma^{i+j}\,\phi(V)) = \gamma^{-k} V = \phi(W).$$

This shows that $V, \phi(W) \in X_r^\partial$. Since we have assumed X_k exists and is not a face, *i.e.*, $k \notin \{0, i, j\}$, X_r cannot be a face incident to V. Hence X_r^∂ must be an edge E' running from V to $\phi(W)$ and X_{-r}^∂ must be the edge $\phi(E')$ running from $\phi(V)$ to W.

The diagram of this situation, as viewed from above, is a ϕ-invariant parallelogram with vertices V, W, $\phi(V)$ and $\phi(W)$, all of which are splendid, see Figure 7.2. At each of these vertices the exterior angle of the parallelogram is larger than π, so the convexity of faces of $\partial\Delta$ implies that this exterior angle must comprise two of the three faces touching the given splendid vertex. This means that all of the interior angles must be spanned by exactly one face, say F_s. By the ϕ-invariance of the parallelogram, we would have that $F_s = \phi(F_s) = F_{-s}$, which is impossible for any loxodromic element. □

There is one more type of one-dimensional intersection to rule out.

Proposition 7.8. *Let E be an edge of $\partial\Delta$ connecting a splendid vertex and a corner of $\partial\widehat{\Delta}$ on $\widehat{\mathbb{C}}$. Then there can be no hemisphere X_k for which $X_k^\partial = E$.*

Proof. Let $V = F_i \cap F_j \cap F_{i+j}$ be the splendid vertex, so that $\gamma^{-i-j}(V) = \phi(V)$. Now speaking precisely, E and $\phi(E)$ are arcs in $\mathbb{H}^3$ with one actual endpoint V and the other end proceeding along a geodesic towards infinity. Thus γ^{-k}, which is a homeomorphism of E with $\phi(E)$, must take V to $\phi(V)$. But once again the same fixed-point argument then shows that $i + j = k$, yielding our contradiction. □

Everything is now in place for the main result of this section. For any given trace τ, consider the curve α of Proposition 6.9 which starts outside of Σ_ρ and ends at τ. For the beginning of α, the corresponding domains Δ have boundary consisting of the disjoint faces $F_{\pm 1} = X_{\pm 1}$. In a sufficiently small interval after α crosses Σ_ρ, $\partial\widehat{\Delta}$ will be of type $\{1, 2, 1\}$ and $\partial\Delta$ will have faces $F_{\pm 1}$ and $F_{\pm 2}$ and edges between F_2 and F_1, F_1 and F_{-1}, and F_{-1} and F_{-2}; see Figure 7.3 for an example. Note that all of the edges here connect corners and there are no vertices, hence we can make the empty assertion that all vertices are splendid.

As we continue along α, new faces cannot appear or disappear nor can any edges vanish inside $\mathbb{H}^3$, by Propositions 7.4 through 7.8. Thus the combinatorial type of Δ only changes by the addition of faces which break out of the corners of $\partial\widehat{\Delta}$ – see Figure 7.4 for a picture of the Ford domain with trace $1 + i$ and of its underside, where the hemispheres $X_{\pm 3}$ are about to break out from two corners of $\partial\widehat{\Delta}$. Faces do not disappear entirely when the corresponding sides no longer contribute to $\partial\widehat{\Delta}$ by Proposition 7.8; this Proposition together with Corollary 5.7 imply that the new vertex which is created when a new face appears corresponding to a new side of $\partial\widehat{\Delta}$ is always splendid.

In summary, all along α the vertices remain splendid, no face is ever completely removed and the faces that are added correspond exactly to the sequence of sides which are added to $\partial\widehat{\Delta}$.

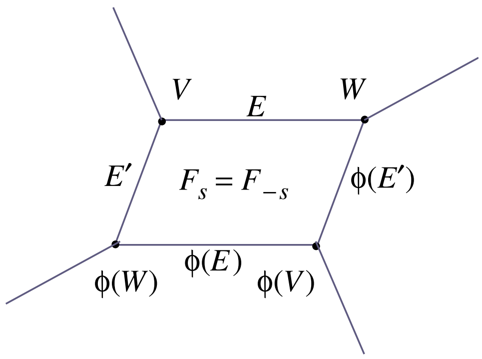

FIGURE 7.2. A parallelogram of edges

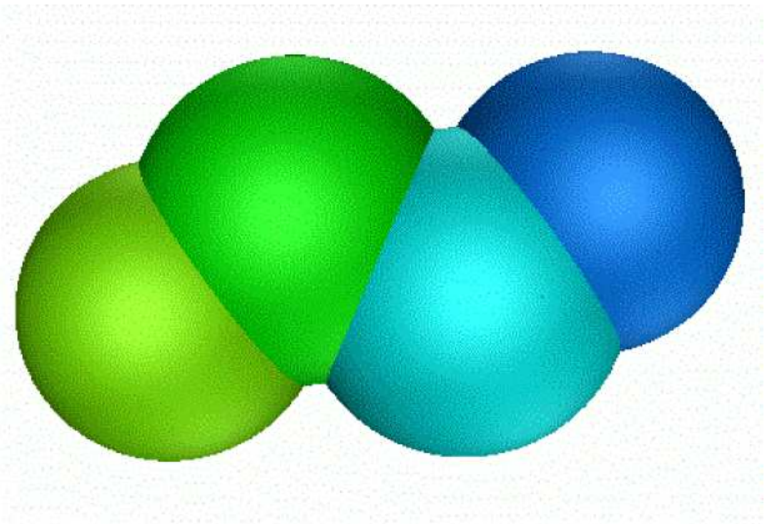

FIGURE 7.3. A domain Δ when the trace τ is of type $\{1,2,1\}$

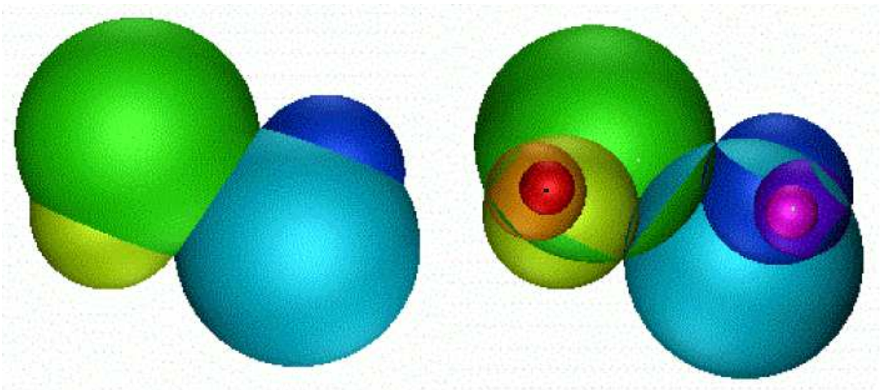

FIGURE 7.4. Top and bottom views of the Ford domain with trace $1+i \in \mathcal{F}_{\{1,2\}}$

Theorem 7.9. *The fundamental domain* Δ *corresponding to a trace* τ *of type* $\{n, n+m, m\}$ *or* $\{n, m\}$ *has as faces exactly those with indices which appear in the Farey denominator sequence starting with* $\{n, m\}$ *and their negatives.*

A simple consequence of this expands on a statement made (without proof) by Jørgensen in [2].

Corollary 7.10. *For any value of the axis distance* $\rho \in (0, \infty]$ *and any positive even integer* N*, there exist traces for which the corresponding domain* Δ *has exactly* N *faces.*

Proof. Let α be a curve in $\mathcal{U}$ which at time 0 is outside Σ_ρ and as $t \to 1$ proceeds in a vertical line down to end at the point $2\cos \pi\xi \in (-2, 2) \subset \mathbb{C}$, for ξ an irrational number. By our results in §6, α passes through infinitely many regions $\mathcal{S}_{\{n,n+m,m\}}$ with n and m always increasing and faces always appearing exactly two at a time. Hence somewhere along α there are traces for which Δ has N faces. $\square$

We conclude with a few more images of fundamental domains in the interior of $\mathbb{H}^3$. First, in Figure 7.5, we show different domains with relatively few sides; then, in Figure 7.6, we show long-distance and close up views of a domain with many sides.

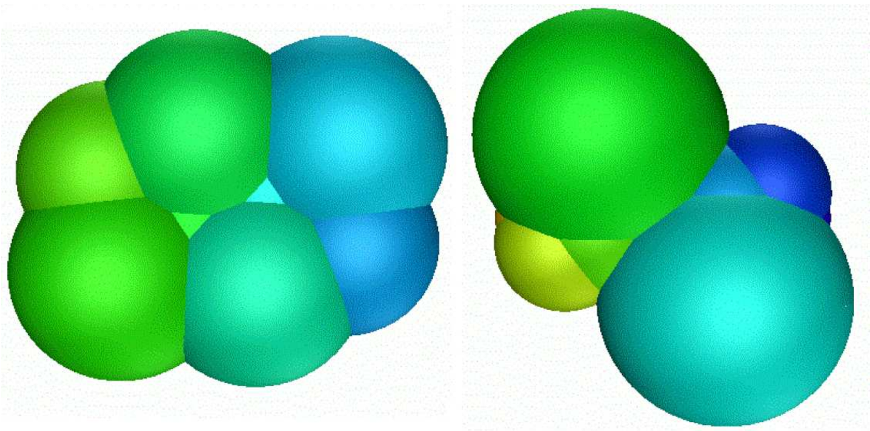

FIGURE 7.5. Examples of fundamental domains inside $\mathbb{H}^3$ with few sides: for trace $1.3 + .3i$ and $1.5 + .5i$

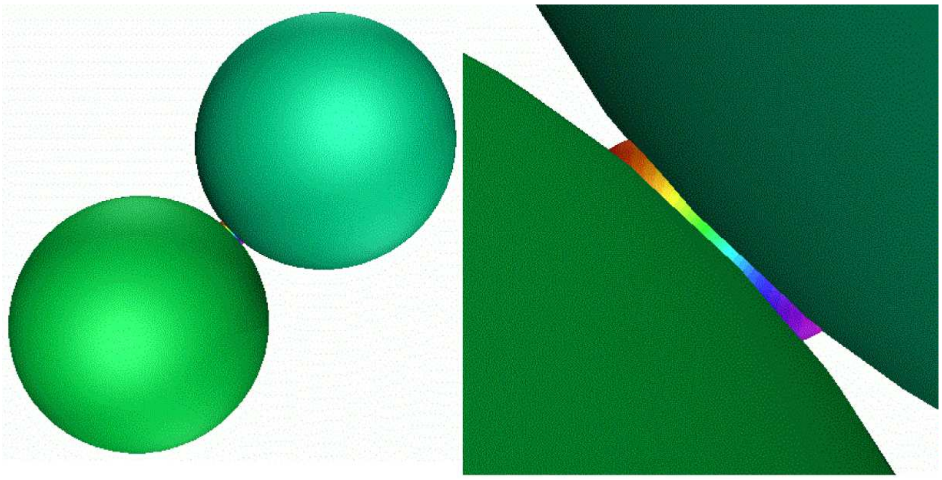

Figure 7.6. An example of a fundamental domain inside $\mathbb{H}^3$ with many sides: trace $.05 + .05i$ from far away and close up.

8. Appendix: related software

In this appendix we describe software which was developed to allow interactive exploration both of individual Ford and Dirichlet domains on $\partial\mathbb{H}^3_{\mathbb{R}}$ and also of how these domains change when the trace of the generator is varied. The results of such explorations motivated much of the approach in previous sections and can greatly clarify the explanations given. In the electronic version of this paper, the software itself is available from the page containing the abstract, while interested readers of the non-electronic version are encouraged to visit at their convenience:

`http://www.ams.org/journal-getitem?pii=S1088-4173(99)00042-9`

The task of displaying Ford and Dirichlet domains corresponding to a given choice of the trace of the generator and of the axis distance is quite simple: the equations (3.3) and (3.5) yield the centers and radii of the isometric and equidistant circles, which can then be drawn in an appropriate window. The only mathematical issue to be dealt with in this simplest aspect of the program is how to decide when enough circles have been drawn, as it is clearly impractical to draw infinitely many. For Ford domains with loxodromic generators, we can proceed as follows. The origin $0 \in \mathbb{C}$ is is contained in all isometric circles with negative indices, so the minimum distance of points on the isometric circle $\widehat{X}_{-1}$ to the origin is

$$\begin{aligned} m_{-1} = R^{iso}_{-1} - \left|C^{iso}_{-1}\right| &= \frac{1}{|\lambda^{-1} - \lambda|} - \left|\frac{\lambda^{-1}}{\lambda^{-1} - \lambda}\right| \\ &= \frac{1 - \left|\lambda^{-1}\right|}{|\lambda^{-1} - \lambda|} = \frac{|\lambda| - 1}{|1 - \lambda^2|}. \end{aligned}$$

Similarly, the maximum distance from points of $\widehat{X}_{-n}$ to the origin obeys

$$M_{-n} = R^{iso}_{-1} + \left|C^{iso}_{-1}\right| = \frac{|\lambda^n| + 1}{|1 - \lambda^{2n}|} \leq \frac{|\lambda^n| + 1}{|\lambda^{2n}| - 1} = \frac{1}{|\lambda^n| - 1}.$$

These isometric circles will not intersect if $M_{-n} < m_{-1}$, hence if

$$\frac{1}{|\lambda^n| - 1} < \frac{|\lambda| - 1}{|1 - \lambda^2|}.$$

This would follow from

$$|\lambda|^n > \frac{|\lambda^2 - 1|}{|\lambda| - 1} + 1,$$

which in turn is a consequence of

$$n \geq 1 + \left\lfloor \frac{\ln\left(\frac{|\lambda^2-1|}{|\lambda|-1} + 1\right)}{\ln|\lambda|} \right\rfloor, \tag{8.1}$$

where as usual $\lfloor x \rfloor$ is the greatest integer less than or equal to x.

Definition 8.1. Given a loxodromic trace τ, let $\lambda = \lambda(\tau)$ be defined in the usual way via (2.9). Then we shall call the right hand side of (8.1) the *maxpow corresponding to* τ. For elliptic traces τ, we will use $\lfloor \mathrm{card}(\Gamma)/2 + 1 \rfloor$ as the maxpow – with ∞ a possible value – while for the parabolic traces $\tau = \pm 1$, we use the maxpow 1.

In practice, any work associated to a trace whose maxpow is large is very computationally intensive. Therefore we introduce an artificial cutoff of 51 for the maxpows we will use in the program.

Lemma 8.2. *No isometric circle with index of absolute value larger than maxpow can contribute to the boundary of a Ford domain on* $\widehat{\mathbb{C}}$.

Unfortunately, the complexity of our expressions (3.3) for the centers and radii of equidistant circles renders inaccessible a similar bound for indices of sides of Dirichlet domains. We have therefore used the Ford maxpow also for Dirichlet domains. This is not known to be correct, but given the compression of the trace plane decomposition we see as we compare the situation for Ford domains in Figure 6.1 to that of Dirichlet domains in Figure 6.2, it seems likely that the Ford maxpow is in fact larger than would be the ideal Dirichlet bound. In any case, the applet has an option to allow the user to override the calculated maxpow with some other value.

One other feature of the program that makes interactive exploration of fundamental domains particularly entertaining is the automatic computation of combinatorial types. When any individual domain is displayed, the combinatorial type of that domain is also shown. This is determined by cutting up all of the circles $\widehat{X}_n$, for $|n|$ less than or equal to the currently selected maxpow, into pieces where they intersect each other and seeing which of the resulting arcs lie outside all of the other circles. (Notice that this is an amount of computation proportional to the square of the maxpow.)

In addition, clicking a button causes the applet to scan the visible portion of the trace plane computing the combinatorial type of the corresponding fundamental domains (each given its associated Ford maxpow) and then coloring the trace plane with different colors for points of distinct combinatorial types. This requires very extensive computation and hence some patience on the part of the user, especially if the real axis, where the maxpow is quite large, is visible in trace plane window.

Of course computer calculations are only of finite precision, and there are two places in the software we are describing where this can affect the output. One is in computing the order of elliptic elements: we do this by taking successive powers of the element until the identity results – but the identity is not likely to be the exact result of a high power of a number with finite precision. Hence we accept that we have found the identity matrix if the corresponding λ has distance squared to $1 \in \mathbb{C}$ of less than 10^{-6}.

While this approximation is rather unsophisticated, it is only relevant when the user selects a trace value in $(-2, 2) \subset \mathbb{C}$ and the program attempts to show the fundamental domain corresponding to an elliptic generator. Most values of τ in this region give generators of infinite order, which will be approximated as having instead large but finite order. The display will thus show many circles $\widehat{X}_n$, clumped together in bands if $\frac{1}{\pi}\cos^{-1}(\tau/2)$ is fairly near a rational of small denominator, but not the infinitely many that should appear. The correct behavior will be displayed, however, when a τ is chosen which agrees to several decimal places with a number $2\cos(\pi q)$ for $q \in \mathbb{Q}$ of small denominator.

The other place that finite precision can cause problems is in the determination of the combinatorial types of fundamental domains. As mentioned above, this involves cutting up many circles $\widehat{X}_n$ into small arcs and seeing when some of these arcs may or may not lie inside other circles. We adopt the convention in these calculations that two points in the complex plane or angles on these arcs are to be considered the same if they differ by at most 10^{-6}. This is not likely to cause any incorrect statements of combinatorial type except perhaps in cases where the maxpow is very large and many circles intersect at nearly the same point, such as when the trace is extremely close to the segment $[-2, 2] \subset \mathbb{C}$.

We conclude by describing specifically the operation of the applet. There are three visible panels when Dirichlet domains have been chosen but only two for Ford domains. These panels are for choosing an axis distance (Ford domains) and a trace of the generator, and then for displaying the corresponding fundamental domain. All of these panels can be zoomed in or out either by clicking on the "+" or "−" buttons or by holding down the right mouse button and dragging up or down in that panel. The trace plane and fundamental domain panels can be translated in the x and y directions by holding down the middle mouse button and dragging in the desired direction. Any panel can be returned to its default magnification and location by clicking its "Reset" button. The axis distance (Ford) and trace can be chosen by clicking the left mouse button in the appropriate panel or by entering in a specific value in the numerical display.

Under the fundamental domain display, there are three pull-down choices. One selects either Dirichlet or Ford domains, another allows the user to override the calculated Ford maxpow with a variety of other values and the last sets the display type to either showing just the circles $\widehat{X}_n$, showing the circles labeled with their indices or showing the circles filled in as disks. Also, over the trace plane display there is a button labeled "Decompose" which causes the combinatorial decomposition of the trace plane to be computed and displayed. This can take some time, so a little patience may be necessary. The decomposition will disappear if the trace plane is zoomed or translated, since such operations cause portions of the trace plane for which the combinatorial type has not be calculated to be shown.

Finally, let us note that because of the symmetries of the trace plane mentioned in §6, we can ignore traces of negative imaginary part. Thus any trace below the real axis will will have its imaginary part set to zero, and any combinatorial decomposition of the trace plane will leave blank that part of the picture.

The applet and the **Java** source code for this applet are available at
`http://www.ams.org/journal-getitem?pii=S1088-4173(99)00042-9`
The code is extensively documented, and can be read directly for comments about how it performs its tasks, or can be run through the **javadoc** program to produce web pages describing the structure of the program.

References

1. A. Beardon, *The geometry of discrete groups*, Springer-Verlag, New York, 1983. MR **85d:**22026
2. T. Jørgensen, *On cyclic groups of Möbius transformations*, Math. Scand. **33** (1973), 250–260. MR **50:**601
3. I. Niven, H. Zuckerman, and L. Montgomery, *An introduction to the theory of numbers*, John Wiley & Sons, New York, 1991. MR **91i:**11001

Department of Mathematics and Statistics, Swarthmore College, Swarthmore, PA 19081
E-mail address: `tad@swarthmore.edu`

Department of Mathematics, Georgetown University, Washington, DC 20057
E-mail address: `poritz@math.georgetown.edu`